2012-06

Inertial Sensor Characterization for Inertial Navigation and Human Motion Tracking Applications

Landry, Leslie M.

Monterey, California. Naval Postgraduate School

NAVAL POSTGRADUATE SCHOOL

MONTEREY, CALIFORNIA

THESIS

INERTIAL SENSOR CHARACTERIZATION FOR INERTIAL NAVIGATION AND HUMAN MOTION TRACKING APPLICATIONS

by

Leslie M. Landry

June 2012

Thesis Advisor:	Xiaoping Yun
Second Reader:	Roberto Cristi

Approved for public release; distribution is unlimited

THIS PAGE INTENTIONALLY LEFT BLANK

REPORT DOCUMENTATION PAGE			*Form Approved OMB No. 0704-0188*
Public reporting burden for this collection of information is estimated to average 1 hour per response, including the time for reviewing instruction, searching existing data sources, gathering and maintaining the data needed, and completing and reviewing the collection of information. Send comments regarding this burden estimate or any other aspect of this collection of information, including suggestions for reducing this burden, to Washington headquarters Services, Directorate for Information Operations and Reports, 1215 Jefferson Davis Highway, Suite 1204, Arlington, VA 22202-4302, and to the Office of Management and Budget, Paperwork Reduction Project (0704-0188) Washington DC 20503.			
1. AGENCY USE ONLY ***(Leave blank)***	**2. REPORT DATE** June 2012	**3. REPORT TYPE AND DATES COVERED** Master's Thesis	
4. TITLE AND SUBTITLE Inertial Sensor Characterization for Inertial Navigation and Human Motion Tracking Applications		**5. FUNDING NUMBERS**	
6. AUTHOR(S) Leslie M. Landry			
7. PERFORMING ORGANIZATION NAME(S) AND ADDRESS(ES) Naval Postgraduate School Monterey, CA 93943-5000		**8. PERFORMING ORGANIZATION REPORT NUMBER**	
9. SPONSORING /MONITORING AGENCY NAME(S) AND ADDRESS(ES) N/A		**10. SPONSORING/MONITORING AGENCY REPORT NUMBER**	
11. SUPPLEMENTARY NOTES The views expressed in this thesis are those of the author and do not reflect the official policy or position of the Department of Defense or the U.S. Government. IRB Protocol number _____N/A_____.			
12a. DISTRIBUTION / AVAILABILITY STATEMENT Approved for public release; distribution is unlimited		**12b. DISTRIBUTION CODE** A	

13. ABSTRACT (maximum 200 words)

Micro-electro-mechanical systems (MEMS) inertial sensors are commonly used in applications such as inertial navigation or human motion tracking. These inertial sensors provide three-dimensional (3D) orientation, acceleration, rate of turn, and magnetic field information. Manufacturers specify both static and dynamic accuracy for the 3D orientation output of MEMS inertial sensors. The dynamic accuracy is in the form of a root-mean-square (RMS) error and is only valid for certain motions, which are not specified. In this thesis, an investigation of the dynamic accuracy of the Xsens Motion Tracker (MTx) inertial sensor was conducted. The yaw or heading dynamic accuracy of the Microstrain DM3-GX3 inertial sensor was also investigated.

A pendulum test apparatus from a previous work was used to test the MTx and GX3. An encoder is installed to the pendulum axis of rotation and provides the reference data needed to calculate the dynamic accuracy of the MTx and GX3.

After a series of motion tests, it was concluded that the MTx was within manufacturer specifications for static accuracy but not for dynamic accuracy. More specifically, the heading or yaw accuracy of the MTx and GX3 did not meet manufacturer specifications under the testing motions chosen in this study.

14. SUBJECT TERMS Micro-electro-mechanical systems, MEMS, Xsens, MTx, dynamic accuracy, human motion tracking, Microstrain, 3DM-GX3-25			**15. NUMBER OF PAGES** 77
			16. PRICE CODE
17. SECURITY CLASSIFICATION OF REPORT Unclassified	**18. SECURITY CLASSIFICATION OF THIS PAGE** Unclassified	**19. SECURITY CLASSIFICATION OF ABSTRACT** Unclassified	**20. LIMITATION OF ABSTRACT** UU

NSN 7540-01-280-5500 Standard Form 298 (Rev. 2-89)
Prescribed by ANSI Std. 239-18

THIS PAGE INTENTIONALLY LEFT BLANK

Approved for public release; distribution is unlimited

INERTIAL SENSOR CHARACTERIZATION FOR INERTIAL NAVIGATION AND HUMAN MOTION TRACKING APPLICATIONS

Leslie M. Landry
Ensign, United States Navy
B.S., United States Naval Academy, 2011

Submitted in partial fulfillment of the
requirements for the degree of

MASTER OF SCIENCE IN ELECTRICAL ENGINEERING

from the

NAVAL POSTGRADUATE SCHOOL
June 2012

Author: Leslie M. Landry

Approved by: Xiaoping Yun
Thesis Advisor

Roberto Cristi
Second Reader

R. Clark Robertson
Chair, Department of Electrical and Computer Engineering

THIS PAGE INTENTIONALLY LEFT BLANK

ABSTRACT

Micro-electro-mechanical systems (MEMS) inertial sensors are commonly used in applications such as inertial navigation or human motion tracking. These inertial sensors provide three-dimensional (3D) orientation, acceleration, rate of turn, and magnetic field information. Manufacturers specify both static and dynamic accuracy for the 3D orientation output of MEMS inertial sensors. The dynamic accuracy is in the form of a root-mean-square (RMS) error and is only valid for certain motions, which are not specified. In this thesis, an investigation of the dynamic accuracy of the Xsens Motion Tracker (MTx) inertial sensor was conducted. The yaw or heading dynamic accuracy of the Microstrain DM3-GX3 inertial sensor was also investigated.

A pendulum test apparatus from a previous work was used to test the MTx and GX3. An encoder is installed to the pendulum axis of rotation and provides the reference data needed to calculate the dynamic accuracy of the MTx and GX3.

After a series of motion tests, it was concluded that the MTx was within manufacturer specifications for static accuracy but not for dynamic accuracy. More specifically, the heading or yaw accuracy of the MTx and GX3 did not meet manufacturer specifications under the testing motions chosen in this study.

THIS PAGE INTENTIONALLY LEFT BLANK

TABLE OF CONTENTS

LIST OF FIGURES

LIST OF TABLES

THIS PAGE INTENTIONALLY LEFT BLANK

LIST OF ACRONYMS AND ABBREVIATIONS

3D	Three-Dimensional
DOF	Degree of Freedom
IEEE	Institute of Electrical and Electronics Engineers
IMU	Inertial Measurement Unit
MEMS	Micro-Electro-Mechanical Systems
MT	Motion Tracker
NI	National Instruments
PC	Personal Computer
RMS	Root-Mean-Square
USB	Universal Serial Bus
VI	Virtual Instrument
XKF	Xsens Kalman Filter

THIS PAGE INTENTIONALLY LEFT BLANK

EXECUTIVE SUMMARY

Inertial sensors are currently produced by many companies for a variety of applications. Inertial sensors based on the micro-electro-mechanical systems (MEMS) technology are smaller in size and can be easily attached to human body segments for personal navigation or human motion tracking. Much work has been done with placing sensors on various parts of the body in an effort to track human motion. This motion tracking could allow for a person to be immersed in a virtual environment instead of simply navigating though the environment with a joystick. These small and compact inertial sensors come with manufacturer specifications for both static and dynamic accuracy. The dynamic specifications are often in the form of root-mean-square (RMS) values and are valid for certain types of motion. The types of motion are not specified by the manufacturer, thus, further testing of these sensors is needed to investigate under what motions the accuracy specifications are valid.

A test apparatus exists that can be used to measure the dynamic accuracy of inertial sensors. The apparatus consists of a pendulum with an optical encoder installed to its rotational axis. The optical encoder provides the reference data for measuring the accuracy of a single rotational axis of an inertial sensor. An inertial sensor can be placed on a platform at the end of the pendulum in such a way to test the three rotation angles individually. The inertial sensor that was under test in this thesis was the Xsens Motion Tracker (MTx). A few tests were also conducted using the Microstrain 3DM-GX3-25.

In order to integrate the MTx into the existing test apparatus, changes to the data collection program were made. These changes were needed to set up communication with the MTx as well as its output settings. A bracket was used to mount the MTx onto the pendulum due to a lack of mounting holes on the sensor. Once the MTx was mounted and the data collection program was running as expected, tests were conducted.

Test methodology developed for the MTx included similar tests to those used in a previous work with an emphasis on the dynamic performance of yaw angle estimation. These tests included free swinging, arbitrary, slow, and stop and hold motions. Tests also

varied in length of time from 15 to 20 seconds all the way to four minutes. The variety of motion tests used were representative of the different types of motion expected in a virtual environment. Results from these tests allowed for investigation of the dynamic accuracy of the MTx.

The pendulum setup permitted only one axis of rotation to be tested at a time. The roll, pitch, and yaw angles of the MTx were all tested individually using the same tests for each rotation angle. The results of the tests conducted on the MTx showed that the roll and pitch angles were within the two degree RMS manufacturer specification for all tests. The roll and pitch angles also were within the defined instantaneous error specification of ±2 degrees during all of the tests. The yaw angle was within specifications for most of the motion tests that were of short duration. For constant back and forth motion tests, in which the pendulum was moved in an arbitrary motion for one minute or longer, the yaw angle began to drift significantly. Once the motion was stopped, the yaw angle returned to within the instantaneous ±2 degree error specification. The MTx yaw angle was found to be within the static accuracy specification but not within the dynamic accuracy specification.

Further yaw angle tests were conducted on the GX3 inertial sensor. The GX3 did not meet accuracy specifications during the yaw tests. The GX3 yaw test results showed that the yaw angle was more accurate during slow motion than during fast motion. These results were consistent with what was seen in the results using the MTx. When the GX3 was moved in a back and forth motion, similar to the test conducted on the MTx, the yaw angle did not drift.

Based on the performance of the MTx under the motion tests conducted in this study, it is possible to use it for human motion tracking. The consideration for drift of the yaw angle during sustained back and forth motion should be taken into account when using the MTx for an application. If constant back and forth motion for a human head can be expected for only a short amount of time, then this sensor could be used for human head motion tracking.

ACKNOWLEDGMENTS

I would like to thank my advisor Professor Xiaoping Yun for introducing me to inertial sensors and guiding me throughout my research with them. He was instrumental in providing me with insight in this subject area. I would also like to thank him for his minimal delay with draft revisions.

I would like to thank James Calusdian, who made it possible for me to complete this work in my short stay at the Naval Postgraduate School. He was always willing to help with a problem I encountered or any questions I had. His timeliness in ordering necessary parts and providing help when difficulties arose played an integral part in what I was able to accomplish.

I would like to thank one of my colleagues, Ensign Michael Moberg, who offered his assistance with designing a mounting bracket needed to attach the sensor to the pendulum. The time he took to design this part in SolidWorks so that I could have it printed on a 3D printer was greatly appreciated. I would also like to thank Daniel Sakoda for his quick turnaround in printing the mounting bracket using a 3D printer.

Lastly, I would like to thank all of my family and friends who have supported me throughout this process.

THIS PAGE INTENTIONALLY LEFT BLANK

I. INTRODUCTION

A. BACKGROUND

An inertial sensor, also known as an Inertial Measurement Unit (IMU), is made up of individual sensing components such as accelerometers, gyroscopes, and magnetometers. All of these individual sensing components are used to provide the orientation of an IMU. The orientation of the IMU can be mapped into a three-dimensional reference frame, such as the *xyz* reference frame, based on rotation about each axis. Typically there is one accelerometer, gyroscope, and magnetometer for each axis of rotation. The respective rotation angles about each axis are known as roll, pitch, and yaw. A schematic of a typical IMU depicting orientation based on rotation about an individual axis is shown in Figure 1.

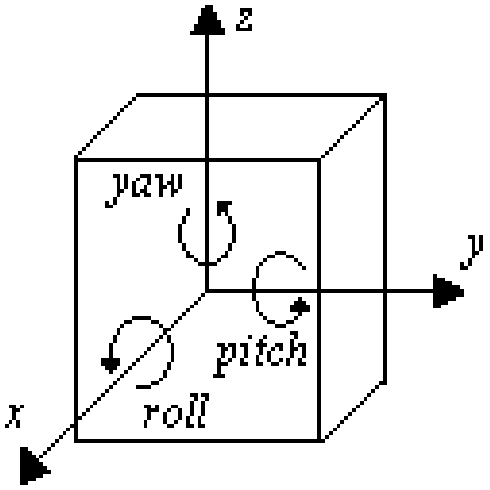

Figure 1. Three-dimensional orientation reference frame.

1. Accelerometers

There are many types of accelerometers, but the principle behind all of them is that they measure acceleration. The acceleration measured can either be static, such as gravity, or dynamic acceleration due to motion. In low-cost, small-size inertial sensors the accelerometers commonly used are Micro-Electro-Mechanical System (MEMS) accelerometers. MEMS technology is used to fabricate accelerometers on a sub-

millimeter scale with a tolerance of one micrometer or less [1]. These smaller accelerometers allow for the IMUs that utilize them to be smaller and more compact. An inertial sensor has an accelerometer devoted to each of the three degrees of freedom (DOF) in order to measure acceleration in the direction of each axis of rotation both due to gravity and motion.

2. Gyroscopes

Gyroscopes measure the rate of turn or angular rate of turn due to motion. MEMS gyroscopes are also commonly used in inertial sensors due to their small size as in the MEMS accelerometers. There is a rate gyroscope for each DOF which aid in calculating the orientation angle with respect to each axis. A simple example of a gyro is a spinning top. When spinning at a particular constant rate, the spinning top will spin upright. Once the top slows down, it begins to spin at an angle instead of perpendicular to the surface. This same thought can be applied to the gyroscopes used in inertial sensors. MEMS gyroscopes utilize the Coriolis Effect to measure angular rate of turn or angular velocity.

3. Magnetometers

Magnetometers measure the strength or direction of either a created magnetic field or naturally occurring one. A magnetometer that measures the magnetic field of the earth can be thought of as a miniature compass. For inertial sensors, magnetometers provide information about heading referenced to magnetic north. Heading can be thought of as rotation about the *z*-axis, or the yaw angle.

B. MOTIVATION

IMUs as well as their individual components are used in a variety of applications today such as robotics or alternatives to GPS location. A very common place that IMUs are used is in virtual reality for human motion tracking. Companies such as Xsens have gone as far as to develop an “Inertial Motion Capture” suit, which uses multiple IMUs attached to a person in the form of a lycra suit in order to track their motion without using

cameras [2]. Individual IMUs can also be used for dead reckoning and calculating position. The formulation for such an algorithm that can track position was demonstrated by James Calusdian in [3].

Though IMUs have a variety of applications, there is at least one aspect of these sensors that should be examined before using them in a particular application. This aspect involves the accuracy of a given IMU. The static and dynamic accuracy of an IMU will dictate whether or not that IMU is suited for an application. The accuracy of an IMU is limited by the quality of the accelerometers and gyroscopes used [4]. Often, the dynamic accuracy of a sensor is given in the form of a root-mean-square (RMS) accuracy value. There is ambiguity as to exactly what is meant by the RMS specification for an IMU because the specification is only valid for certain types of motion. The types of motion for which the RMS dynamic accuracy specification is valid are often not specified by the manufacturer of a particular inertial sensor.

The Institute of Electrical and Electronics Engineers (IEEE) provides a very detailed standard for testing of inertial sensors [5]. Most of the test procedures involve testing individual components of the IMU such as the accelerometer readings. Companies such as InterSense, Microstrain, and Xsens have developed algorithms which calculate orientation of an inertial sensor through the use of accelerometers, gyroscopes, and magnetometers. The details of what the algorithms are doing to calculate orientation data (roll, pitch, and yaw angles) are not known. This leads to a need for testing of the orientation output calculated by these algorithms.

C. PREVIOUS WORK

There are different methods for evaluating the accuracy of an inertial sensor. The method used relates to the intended application of an inertial sensor. In [6], the performance of low cost MEMS inertial sensors was characterized. The intended application of the MEMS inertial sensors was indoor and outdoor navigation. Due to the application, the accuracy of the raw accelerations and angular rotations was the focus during testing. The reference used for accuracy testing was a high precision survey grade IMU.

Similar accuracy testing has also been conducted for orientation data of a MEMS inertial sensor. In [7], a prototype inertial sensor, ETHOS, was constructed and another, more precise IMU was used to characterize its accuracy. The intended application of ETHOS was for tracking of human movement and testing involved both static and dynamic conditions.

A group of inertial sensors was tested in [8], which also involved static and dynamic motions. In the study four inertial sensors were mounted to a plastic plate and put through motion tests. The accuracy of the sensors was based on the relative orientation of the sensors to each other. There was no external reference used to characterize the inertial sensors.

Contrary to these accuracy tests, a test apparatus was developed with an external reference to test the accuracy of inertial sensors. In [9], Jonathan Shaver tested the orientation data of a Microstrain inertial sensor by building a pendulum with an encoder installed to its axis of rotation. The encoder provided the reference data needed to investigate the accuracy of the Microstrain sensor. His work was extended by Jeremy Cookson in [10], who built a less flexible pendulum with a higher precision encoder which was used to test two Microstrain inertial sensors.

D. GOALS

The goal of this thesis is to use the existing test apparatus from [10] to test the Xsens miniature inertial 3DOF Orientation Tracker. In particular, the dynamic accuracy of the Motion Tracker (MTx) will be investigated in order to determine both RMS error as well as instantaneous error of orientation data.

The intended application for the MTx is human head motion tracking in a virtual environment. The previously tested Microstrain inertial sensors were intended for use in human foot motion tracking. The test methodology in this study will be similar to the test methodology used in [10] with the exception of impact testing. The impact testing previously used mimicked motion of a human foot while walking. Since the intended application for the MTx is head motion tracking and no impact is expected, the impact tests are not used in this study. The tests that are used vary in type of motion and

duration. Additionally, the intended application of head motion tracking involves mainly yaw motion. An emphasis of this thesis is on evaluation of the dynamic performance of the yaw angle.

Based on the results from all of the tests run with the MTx, a determination on whether or not this sensor is suitable for human head motion tracking will be made.

THIS PAGE INTENTIONALLY LEFT BLANK

II. THE XSENS MTX

The Xsens MTx is an IMU that tracks and yields three-dimensional (3D) orientation as well as raw data. The raw data includes 3D acceleration, 3D rate of turn, and 3D earth magnetic field. It comes with everything needed to get started immediately using the sensor, such as its own software to collect data (MT Manager), which can be installed on a Personal Computer (PC), and a Universal Serial Bus (USB) connection cable to allow easy connection to a PC. Documentation is also provided to give the user the ability to utilize all of the features of the sensor. The sensor can be used in fields such as biomechanics, exercise, sports, virtual reality, animation, and motion capture [11]. The MTx comes in plastic housing and is shown in Figure 2.

Figure 2. The Xsens MTx.

A. FEATURES

The MTx has unique features such as the Xsens Kalman Filter (XKF), which allows the user to select an operating scenario based on motion or environmental conditions. The five scenarios for the XKF and the corresponding sensing components used for each scenario are shown in Table 1. The IMU column in Table 1 corresponds to the use of accelerators and gyroscopes. These scenarios allow the XKF algorithm to make assumptions about motion or the environment to calculate orientation data accurately.

Since a possible application for this sensor is human head motion tracking, either the human or human large acceleration scenarios are suitable. In this thesis, only the human large acceleration XKF scenario was used.

Table 1. XKF scenarios (From [11]).

XKF-3 Scenario	IMU	Magnetometer
Human	●	●
Human_large_accel	●	●
Machine	●	●
Machine_nomag	●	
Marine	●	●

1. Components

The XKF uses sensor readings from the accelerometers, gyroscopes, and magnetometers that the MTx houses. The accelerometers used by the MTx are MEMS solid state accelerometers with capacitive readout. The gyroscopes used to measure the rate of turn are MEMS solid state monolithic beam structured gyroscopes with capacitive readout. Finally, the magnetometers are thin film magnetoresistive sensors that utilize the magnetic field of the earth for orientation purposes.

The MTx also has temperature sensors onboard. These sensors are used to measure the temperature of the other sensors the MTx houses. The temperature readings from the temperature sensors are used to compensate for inaccuracies in sensor readings due to increasing temperatures during operation. Compensating for component inaccuracies allows for a more accurate calculation of the orientation output.

2. Software Package

The MTx comes with user friendly software for easy data logging. This software is called Xsens MT Manager. MT Manager allows for easy initialization of desired output

settings such as sampling frequency or orientation data in the form of Euler angles or quaternions. This software is a good way to become familiar with all of the features of the MTx and to log data. In this thesis, the MT Manager software was only used for static (no movement) testing to see if MTx readings of interest tended to drift over a long period of time. MT Manager was not used for testing the dynamic accuracy of the orientation data of the MTx because of the difficulty of collecting truth data from the pendulum encoder using this software. Without the truth data, the dynamic accuracy of the MTx cannot be calculated.

B. PERFORMANCE SPECIFICATIONS

Xsens provides performance specifications for the orientation output of the MTx. These performance specifications are listed in Table 2. The dynamic accuracy specification in Table 2 was the focus of this thesis. The dynamic accuracy specification is a RMS value and is only valid for certain types of motion. Xsens provides no documentation that specifies what type of motion the RMS specification holds.

The RMS value specified is an average accuracy over an unspecified amount of time and does not address instantaneous accuracy of the MTx. Depending on the intended application of the MTx, we may not need knowledge of the instantaneous accuracy. For example, in human motion tracking an average accuracy over time is not sufficient. The maximum value of the error at every time sample is needed for accurately tracking human motion.

Table 2. MTx performance specifications (From [11]).

Specification		Notes:
Angular Resolution:	0.05°	1 standard deviation of zero-mean random walk
Static Accuracy (roll/pitch):	0.5°	
Static Accuracy (heading):	1.0°	
Dynamic Accuracy:	2.0° RMS	may depend on type of motion

C. ORIENTATION

The MTx has various data output settings. Orientation data can be collected in the form of a rotation matrix, Euler angles, or quaternions. The MTx can also provide raw inertial data from the accelerometers, gyroscopes, and magnetometers. The MTx orientation output used in this thesis was the quaternion. Rotation about an axis follows the right hand rule convention, meaning clockwise rotation is positive. The data outputs are single-precision, floating-point values as defined by the IEEE 754 standard. The MTx uses an earth fixed coordinate system which is shown in Figure 3. The MTx rotation angles are all zero when the sensor coordinate frame is aligned with the earth fixed coordinate frame. More specifically, when the positive *x*-axis is pointing in the direction of magnetic north and the *y*-axis is pointing west, then there is zero rotation about all of the axes.

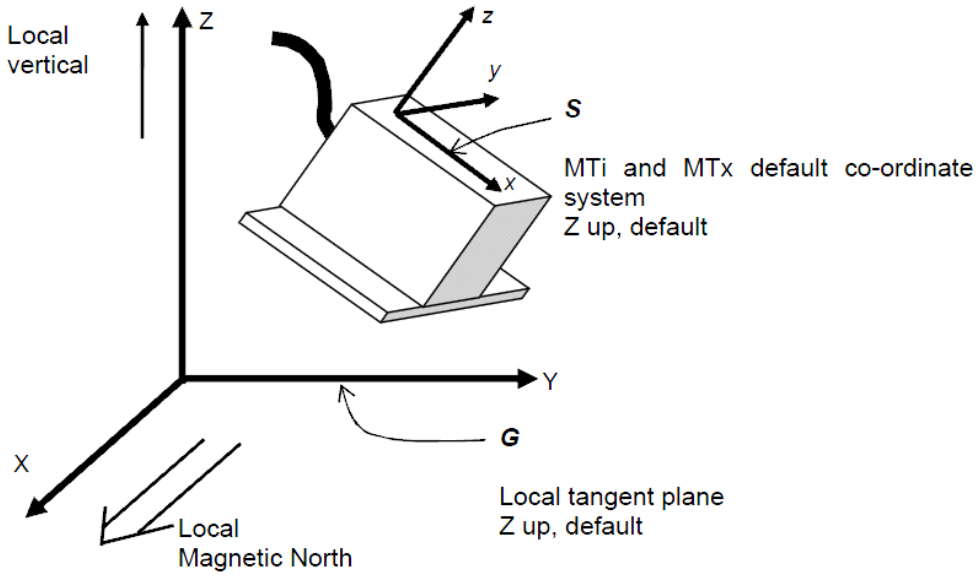

Figure 3. MTx coordinate system reference (From [11]).

D. COMMUNICATION

There are three options for communication with the MTx. The MTx is capable, given the appropriate cable, to communicate using USB or standard RS-232 or RS-485 serial communication. In this thesis, RS-232 serial communication was used to collect data from the MTx. Before data collection could occur, the MTx needed to be configured.

This configuration involved initializing the sensor for the desired orientation output in the form of quaternions as well as setting up the sensor to operate in polling mode. The RS-232 messages needed to configure the MTx output settings are outlined in detail in [12].

In this chapter, the MTx was discussed in detail. The hardware and software features of the sensor were introduced as well as relevant manufacture specifications. Also, the MTx orientation reference frame was presented. In Chapter III, data collection and test methodology are discussed. The first part of Chapter III addresses the software needed to collect data from the MTx. The second part of Chapter III explores the motion tests performed on the MTx.

THIS PAGE INTENTIONALLY LEFT BLANK

III. DATA COLLECTION

LabVIEW was used to communicate with and collect data from the MTx. LabVIEW is software developed by National Instruments (NI), which allows a user to graphical build a program. It is easy to learn and contains many tools for measurement and control systems. The data collection program was developed in LabVIEW on a PC and deployed to a NI CompactRIO Real-Time controller, the NI cRIO-9012. The real-time controller executes the data collection program and allows for data to be collected with minimal latency. The real-time controller has less overhead than a PC, which allows for synchronization of the data collected. The controller communicates with the MTx through its RS-232 port. The LabVIEW programming used to collect the truth data from the encoder on the pendulum was accomplished in [10]. The only LabVIEW programming developed in this thesis was for communication with and data collection from the MTx.

A. LABVIEW PROGRAMS

LabVIEW programs are called Virtual Instruments (VI). The VI used for data collection is shown in Figure 4. A "subVI" is a function within a VI. The "subVIs" developed specifically for the MTx are indicated in Figure 4. The data collection VI has a large grey box, which represents a while loop function. Within the loop are subVIs that are executed during each iteration of the loop. The subVI labeled "Encoder Angle" collects the encoder data. The subVI labeled "Get MTx" collects the orientation data from the MTx. The outputs from both subVIs are then combined in an array. This loop continuously executes until the program is stopped. Once the program is stopped, the data array is written into a text file, which is labeled text.txt in Figure 4. The MTx subVI labeled MTx Serial Int initializes communication with and output settings of the MTx before the while loop is executed.

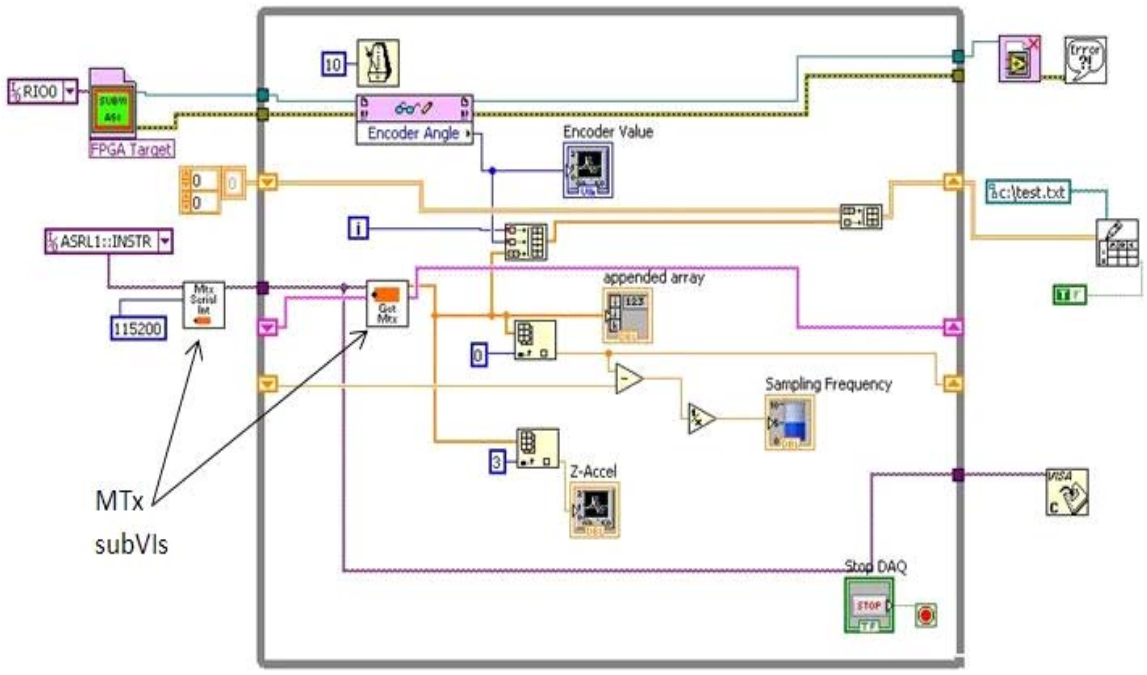

Figure 4. LabVIEW program for data collection from the MTx.

1. MTx Serial Initialization subVI

The MTx Serial Initialization subVI sets up serial communication with the MTx and also sets the desired output settings. The full block diagram of the subVI for initialization of the MTx is in the Appendix. The inputs to the subVI are the CompactRIO RS-232 port that the MTx is connected to and the baud rate of the MTx.

Once the serial port and baud rate were provided to the subVI, the serial communication with the MTx was established. Following the serial port setup, the MTx was put into a configuration state. Next, the output mode for the MTx was set to calibration and orientation data. The calibration data includes readings from the three accelerometers, gyroscopes, and magnetometers the MTx houses. Lastly, the orientation output was set to quaternion, and the MTx was put in polling mode. Polling mode allows the user to request data at any time. The ability to request data at arbitrary times was needed due to the existing program. The original LabVIEW program did not collect data at a fixed sampling interval due to the memory allocation setup for the CompactRIO. A fixed sampling interval was not needed for accuracy testing, and further investigation into

fixing this issue was not pursued. Once initialization of the MTx output settings was completed, the sensor was put into the measurement state. In the measurement state, the sensor simply waits until data is requested and sends the output data with minimal latency. The serial port that the MTx was connected to on the CompactRIO was the only output of the initialization subVI.

2. MTx Data Collection subVI

The MTx Data Collection subVI requests the data output from the MTx that was set up in the initialization subVI. The full block diagram for this subVI is in the Appendix. The only input to the subVI was the serial port that the MTx was connected to on the CompactRIO. Using this serial port, we request the output data from the MTx. There is a three millisecond delay between writing to and reading from the serial port. The length of the data was then compared to the expected length of the output data. The expected length, or number of bytes in the RS-232 message, can easily be calculated based on the standard message structure and output settings for the MTx. If the length of the byte stream from the serial port was not the expected length, then the data was discarded. If the length of the message was the expected length, then the byte stream was passed through for further processing.

The header of the data message was then discarded and the remainder of the message separated into segments that correspond to individual data fields. All of the data fields were four bytes long and were converted to single-precision floating point values. The sample count was the only data field that was two bytes long, and it was converted into an unsigned integer value. All of the converted values were put into an array and passed out of the subVI.

3. Overview of Data Collection Program

Once the MTx subVIs were added to the existing program, data collection commenced. This program initialized the desired output data of the MTx as well as communication with the MTx and optical encoder on the pendulum. After communication was established, the program entered a while loop where the truth data from the encoder and the inertial sensor data were collected, processed, and stored. When

the program was stopped, all of the data collected was saved into a text file. A simple functional block diagram of how this program worked is shown in Figure 5.

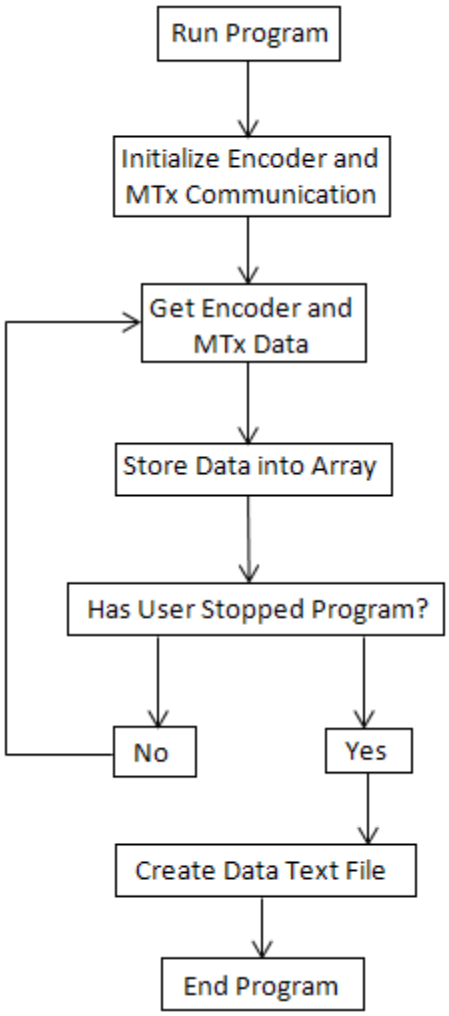

Figure 5. LabVIEW program functional block diagram.

B. PHYSICAL TEST SETUP

Only one axis of rotation of the sensor was tested at a time. The test apparatus and sensor were oriented in such a way that the axis which is parallel to the axis of rotation of the pendulum was the rotation axis tested. This setup of the sensor and pendulum means that the other two axis of rotation should remain constant because the sensor is only rotating about one axis. The pendulum and sensor setup for testing rotation about the *x*-

axis, or roll angle, of the sensor is shown in Figure 6. All tests conducted to test the roll angle were done with the test apparatus setup shown in Figure 6.

Figure 6. Test apparatus setup to test the roll angle.

To test rotation about the *y*-axis, or pitch angle, the sensor position on the pendulum in Figure 6 was changed. Since the *y*-axis is the axis to be tested, then the sensor must be positioned on the pendulum such that the *y*-axis is parallel to the axis of rotation of the pendulum. The apparatus setup for testing the pitch angle of the sensor is shown in Figure 7. All tests conducted to test the pitch angle were done with the test apparatus setup shown in Figure 7.

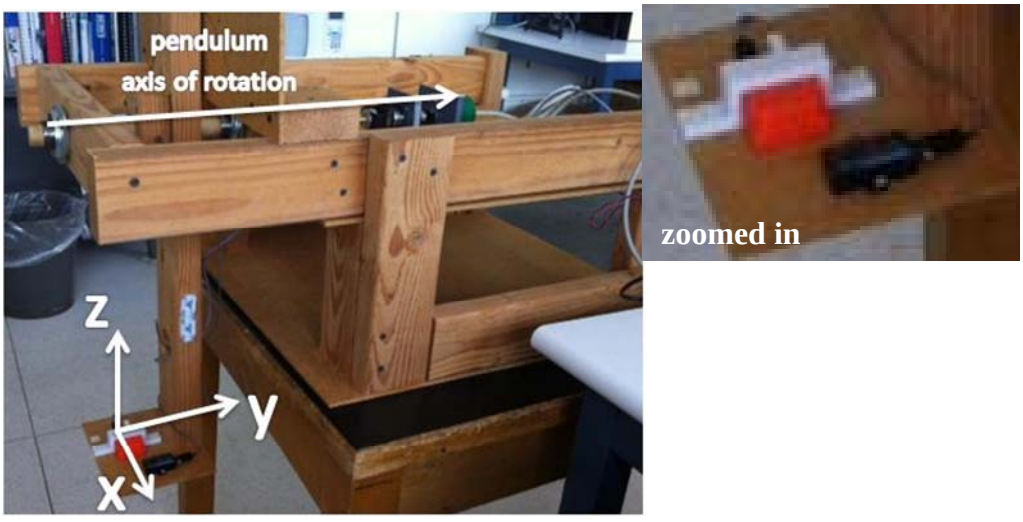

Figure 7. Test apparatus setup to test the pitch angle.

To test rotation about the *z*-axis or the yaw angle, the pendulum was tilted up and the sensor position changed from Figure 7. The sensor was positioned such that the *z*-axis was parallel to the vertical rotation axis of the pendulum. The apparatus setup for testing the yaw angle of the sensor is shown in Figure 8. All tests conducted to test the yaw angle were done with the test apparatus setup shown in Figure 8.

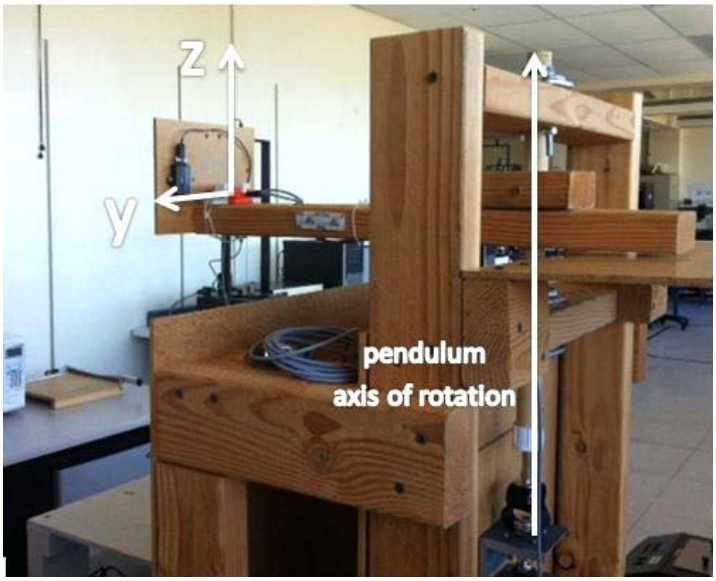

Figure 8. Test apparatus setup to test the yaw angle.

C. TEST METHODOLOGY

The testing of the MTx focused on dynamic vice static testing in order to investigate the dynamic accuracy of the sensor. Similar tests performed in [10] are used to test the MTx as well as new tests. It is impossible to test the dynamic accuracy of the sensor fully because that would require testing the sensor under all possible motions. Instead, a number of different motion tests that are representative in the intended virtual environment application were used in an effort to characterize the dynamic accuracy.

All of the tests started by running the test program. For the first two to three seconds when the program was started and collecting data, the pendulum was not moved. After the first two to three seconds, a motion test took place. The length of each motion test varied from 10 to 20 seconds. Once the test was finished and the pendulum was not moving, the program ran for another five seconds and then was stopped. In an effort to

see the dynamic accuracy over a longer amount of time, some longer tests were also run on the MTx. Descriptions of each test run on the MTx are outlined in the following sections.

1. Free Swing Tests

Free swing tests conducted on the MTx involved rotating the pendulum to a reference angle, either the right or left, and releasing the pendulum to swing freely until it stopped swinging. The reference angles that the pendulum was released from are shown in Figure 9. Due to the position of the pendulum during yaw angle tests, the free swing yaw angle tests were conducted so that the motion of the pendulum mimicked the free swing motion of the roll and pitch angle free swing tests.

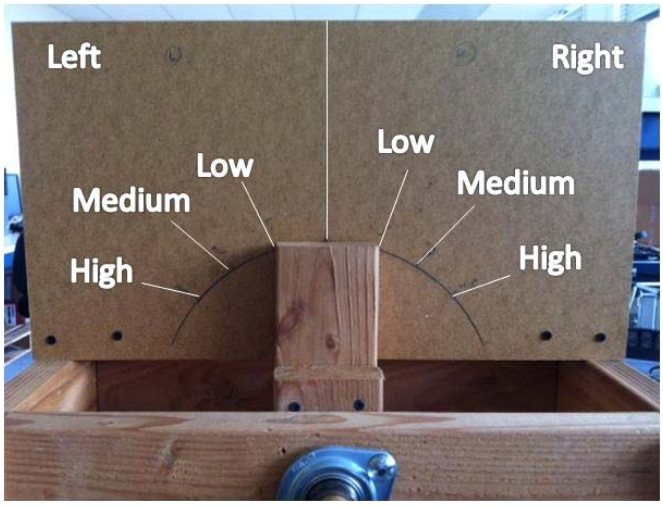

Figure 9. Reference angles for the free swing tests.

The encoder data collected for low, medium, and high free swing tests are shown in Figures 10, 11, and 12. From Figure 10, it is seen that the pendulum was pushed by hand from the zero degree angle to about 17 degrees (corresponding to the low reference angle shown in Figure 9) during the five to seven second period. The pendulum was then released and underwent a free swing period and finally stopped at the initial zero degree position. Similar pendulum behaviors for the medium and high reference angles are shown in Figures 11 and 12. The medium reference angle is about 33 degrees, while the high reference angle is about 50 degrees.

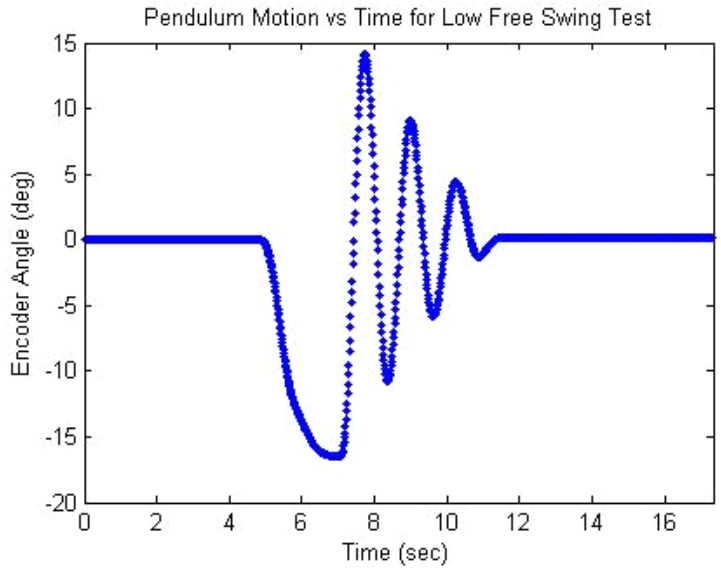

Figure 10. Encoder angle for the low free swing test.

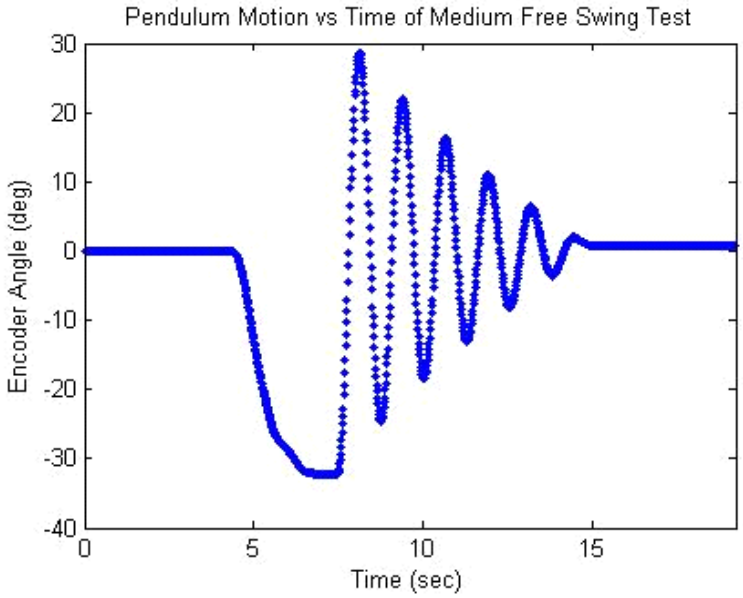

Figure 11. Encoder angle for the medium free swing test.

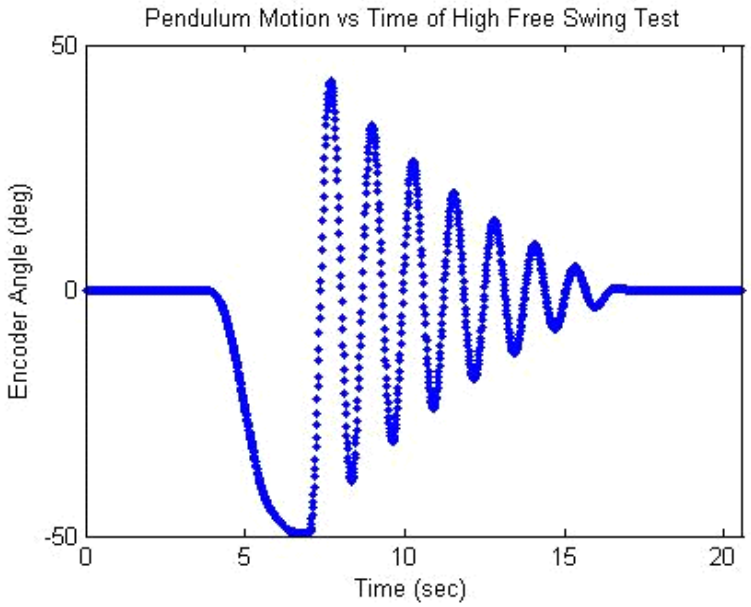

Figure 12. Encoder angle for the high free swing test.

2. Arbitrary Movement Tests

For arbitrary movement tests the pendulum was moved randomly through slow, fast, or stopping motions. No effort was made to have the same sequence of motions for testing of the roll, pitch, and yaw. The random movement lasted 15 to 20 seconds. Longer arbitrary movement tests were also conducted to investigate the accuracy of the orientation angles over a longer duration of time. The encoder data collected for an arbitrary movement test is shown in Figure 13.

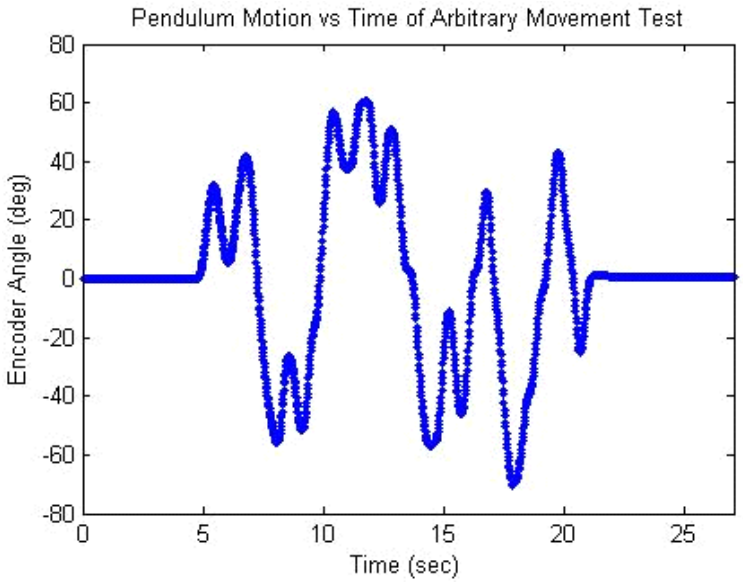

Figure 13. Encoder angle for the arbitrary movement test.

3. Slow Movement and Stop and Hold Tests

For slow movement tests, the pendulum was moved continuously at a slower motion than the free swing tests. The pendulum was moved back and forth slowly for about 10 to 20 seconds. For stop and hold tests, the pendulum was moved to a position and held there for about 10 seconds. After holding the pendulum in one place for about 10 seconds, it was moved to another position and left there for another five seconds. The encoder data collected for slow movement and stop and hold tests is shown in Figures 14 and 15.

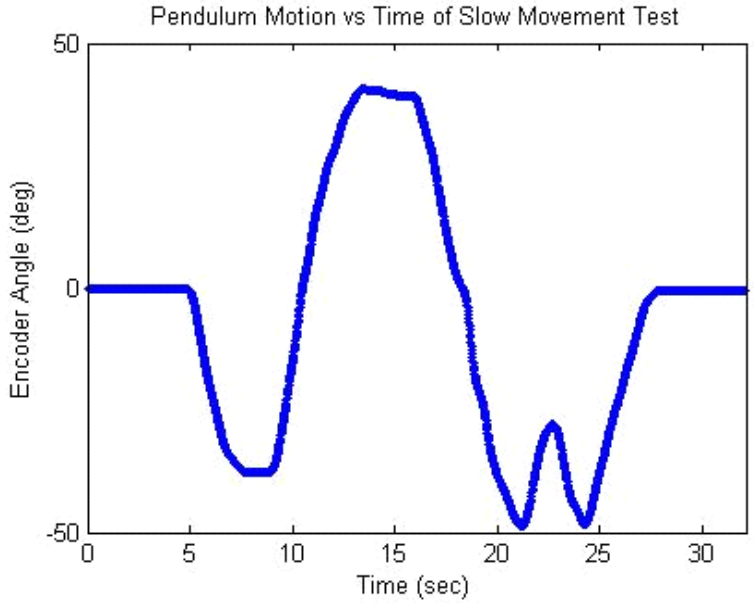

Figure 14. Encoder angle for the slow movement test.

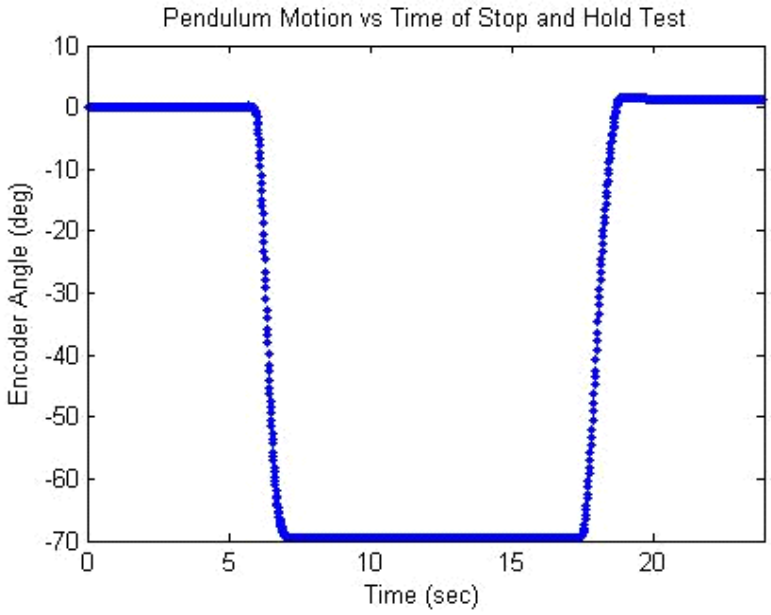

Figure 15. Encoder angle for the stop and hold test.

4. Additional Yaw Tests

There were three additional yaw tests performed on the MTx. The first test performed was a static test. In the static test, the MTx was not moved for about

30 minutes. The purpose of this test was to see if the yaw angle tended to drift over time. The second test was a longer version of the arbitrary movement test. This longer test focused on moving the pendulum constantly back and forth. This test lasted about three minutes. The third test performed was a period of arbitrary movement followed by no motion of the pendulum. The movement portion of the test lasted about one minute, and then the pendulum was left static for about three minutes.

Three additional yaw tests were also conducted on the Microstrain 3DM-GX3 used in [10] to further investigate the yaw accuracy of a different inertial sensor. The first test consisted of slow movements with stationary periods between each movement. The last two tests conducted were arbitrary movement tests for both a short and long period of time.

5. Test Matrix

A test matrix was created to keep track of all tests performed and is shown in Table 3. The blank spaces in the matrix represent individual tests.

Table 3. Test matrix.

MTx TESTS	ROLL	PITCH	YAW
Free Swing From Left Low			
Free Swing From Left Medium			
Free Swing From Left High			
Free Swing From Right Low			
Free Swing From Right Medium			
Free Swing From Right High			
Arbitrary Movement			
Slow Movement			
Stop and Hold			
Longer Arbitrary M.			

MTx ADDITIONAL TESTS	YAW
Static	
3 Minute Arbitrary M.	
Long Arbitrary with Stop	

GX3 ADDITIONAL TESTS	YAW
Slow Movement	
Short Arbitrary	
Long Arbitrary	

D. DATA CONVERSIONS

Processing of output text files from the LabVIEW data collection program was done in a MATLAB script file. The encoder output and the quaternion orientation output of the MTx were converted to angles in order to make comparisons.

1. Encoder

The 16-bit optical encoder on the pendulum outputs counts. The output from the encoder had to be converted to an angle in degrees in order to make comparisons to the roll, pitch, and yaw angles of the MTx. The conversion factor is

$$\left(\frac{360\text{deg}}{1\,\text{rotation}}\right)\left(\frac{1\,\text{rotation}}{2^{16}\text{counts}}\right) = 0.00549\ \text{deg/count}. \tag{1}$$

2. Orientation

The orientation data collected from the MTx was in the form of a quaternion and needed to be converted to roll, pitch, and yaw angles. The format for a quaternion is

$$q = \begin{bmatrix} q_0 \\ q_1 \\ q_2 \\ q_3 \end{bmatrix} \tag{2}$$

where q_0, q_1, q_2, and q_3 are real number components. The components of a quaternion are further divided into parts. The scalar part is q_0, and the vector part includes q_1, q_2, and q_3 [13].

The quaternion can be converted to roll, pitch, and yaw using the conversions provided in [11]

$$\text{roll} = \tan^{-1}\left(\frac{2q_2q_3 + 2q_0q_1}{2q_0^2 + 2q_3^2 - 1}\right) \tag{3}$$

$$\text{pitch} = \sin^{-1}(2q_1q_3 - 2q_0q_2) \tag{4}$$

and

$$\text{yaw} = \tan^{-1}\left(\frac{2q_1q_2 + 2q_0q_3}{2q_0^2 + 2q_1^2 - 1}\right). \quad (5)$$

IV. RESULTS

In this chapter, the results from all of the tests described in Chapter III are presented. First, the error calculations that were done for each test are defined. After this, all of the error plots for each test are displayed as well as a plot of roll, pitch, and yaw in order to see if the two rotation angles not under test remained constant. The plots of the roll, pitch, and yaw angles are referred to as cross-talk plots. After the test results are shown, observations about the results are made to conclude this chapter.

In order to present the results, the encoder angle data and MTx rotation angle under test needed to be aligned for each test. This alignment was necessary because after the encoder count data was converted to an angle in degrees, the encoder angle data was a shifted version of the MTx roll, pitch, or yaw angle data. This shift was not with respect to time but instead with respect to the angle under test. In order to reconcile the angular shift, an average of the last ten points of the MTx rotation angle under test was calculated before the motion test started. The calculated angle was either added or subtracted to the encoder data for that respective test. No timing adjustments were needed for the MTx data collected. The GX3 data was aligned with the encoder angle data in the same way as the MTx data. Unlike the MTx, the GX3 required timing adjustments. The GX3 data timing adjustments were made similar to those made in [10]. These timing adjustments included aligning the peaks of the encoder angle data and GX3 yaw angle data for each test.

A. ERROR CALCULATIONS

Xsens provides a RMS dynamic accuracy specification for the MTx of two degrees in [11]. The RMS of a set of observations $x_1, x_2, \ldots, x_n$ is defined as [14]

$$RMS = \sqrt{\frac{x_1^2 + x_2^2 + x_3^2 + \cdots + x_n^2}{n}}. \tag{6}$$

Given the definition of RMS, the dynamic accuracy RMS value for a single motion test is

$$RMS\ error = \sqrt{\frac{(s[1]-a[1])^2 + (s[2]-a[2])^2 + (s[3]-a[3])^2 + \cdots + (s[n]-a[n])^2}{n}} \quad (7)$$

where $s[i], i = 1,\ldots,n$ are the MTx rotation angles under test, $a[i], i = 1,\ldots,n$ the encoder angles, and n the data set length. The RMS error calculation only used the data when the MTx was in motion because it is a dynamic performance specification. The RMS error is displayed on all of the error plots.

All of the error plots show instantaneous error points for the entire test. For the intended application of the MTx, ±2 degrees instantaneous accuracy was also investigated. This accuracy specification was placed on all of the error plots in the form of red lines at ±2 degrees.

B. MTX RESULTS

This section contains all of the results of the tests described in Chapter III conducted on the MTx. The results are displayed in the form of error plots that are also annotated with the RMS error value for that respective test.

1. Free Swing

This section contains the results of the free swing tests described in Chapter III for roll, pitch, and yaw angles of the MTx.

a. Roll

The roll accuracy of the MTx for the free swing tests at low, medium, and high reference angles is shown in Figures 16, 17, and 18. There are two plots for each figure, one starting the free swing test from the left and the other from the right. From Figure 16, we see that the maximum instantaneous roll angle error is about one degree. The RMS errors are 0.5045 and 0.4816 for the tests started from left and right, respectively. Consequently, the roll error for the low free swing test met the manufacturer RMS dynamic accuracy specification and the instantaneous accuracy specification.

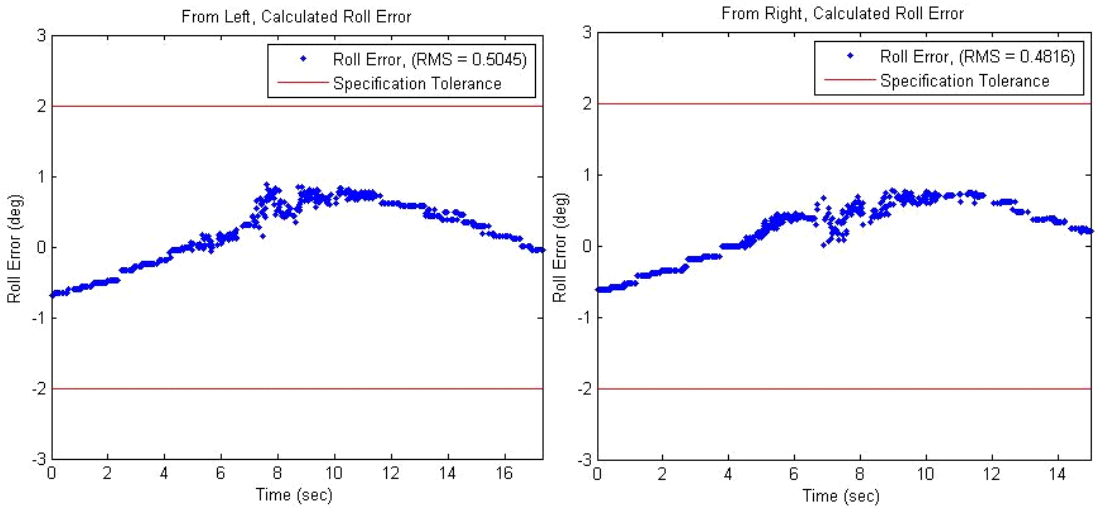

Figure 16. MTx roll accuracy for the free swing low reference angle test.

Similarly, the roll error for the medium free swing test starting from the right and left in Figure 17 met the manufacturer RMS dynamic accuracy specification and the instantaneous accuracy specification. The instantaneous error values were larger for the free swing test starting at a medium reference angle than starting at a low reference angle. This is because the higher the starting reference angle the faster the pendulum initially swings. Faster motion is more difficult for the sensor to track than slower motion and resulted in larger instantaneous errors in the medium reference angle tests.

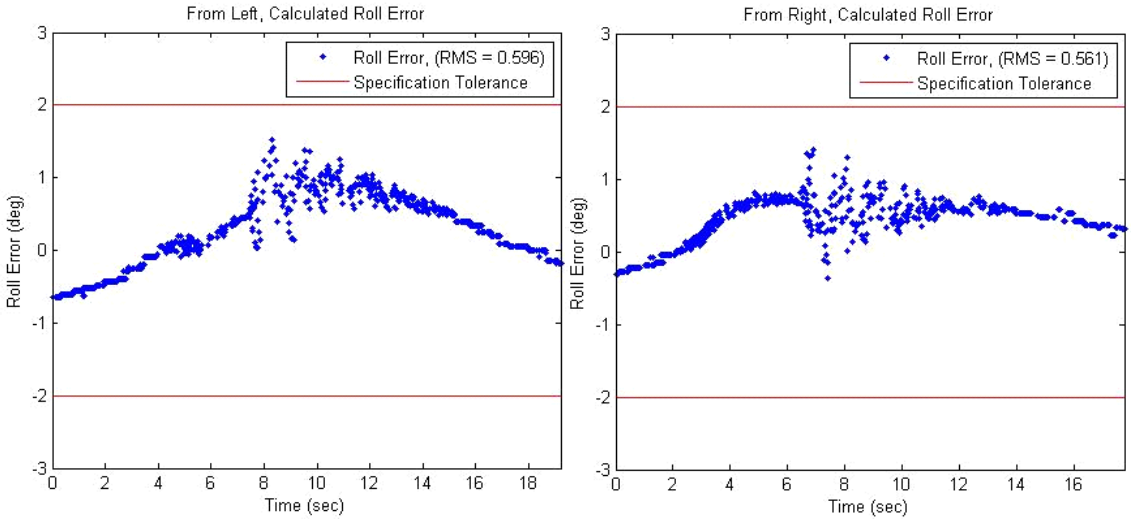

Figure 17. MTx roll accuracy for the free swing medium reference angle test.

Just as in the low and medium reference angle tests, the roll error for the high free swing test shown in Figure 18 met both error specifications. The instantaneous error reached larger values than was seen in both the low and medium reference angle tests. The larger instantaneous error values were a result of the faster motion of the pendulum for the higher starting angle.

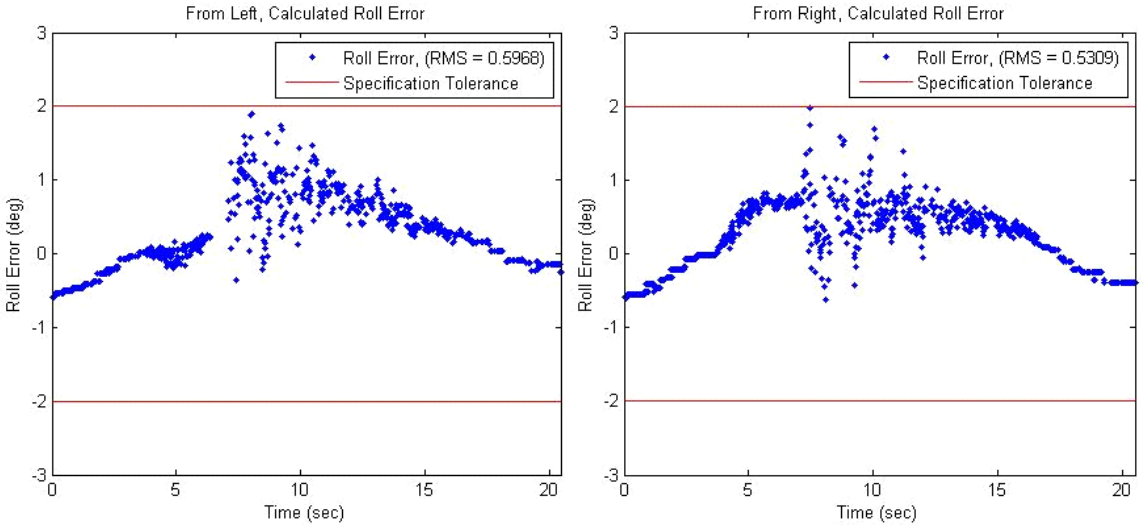

Figure 18. MTx roll accuracy for the free swing high reference angle test.

b. Pitch

The pitch accuracy of the MTx for the free swing tests at low, medium, and high reference angles is shown in Figures 19, 20, and 21. The results for the pitch accuracy were similar to those observed for the same tests performed on the roll angle. The RMS error was within the manufacturer specifications as well as the instantaneous error specifications for all of the tests. As the starting reference angle increased, the instantaneous error values increased due to the faster motion of the pendulum.

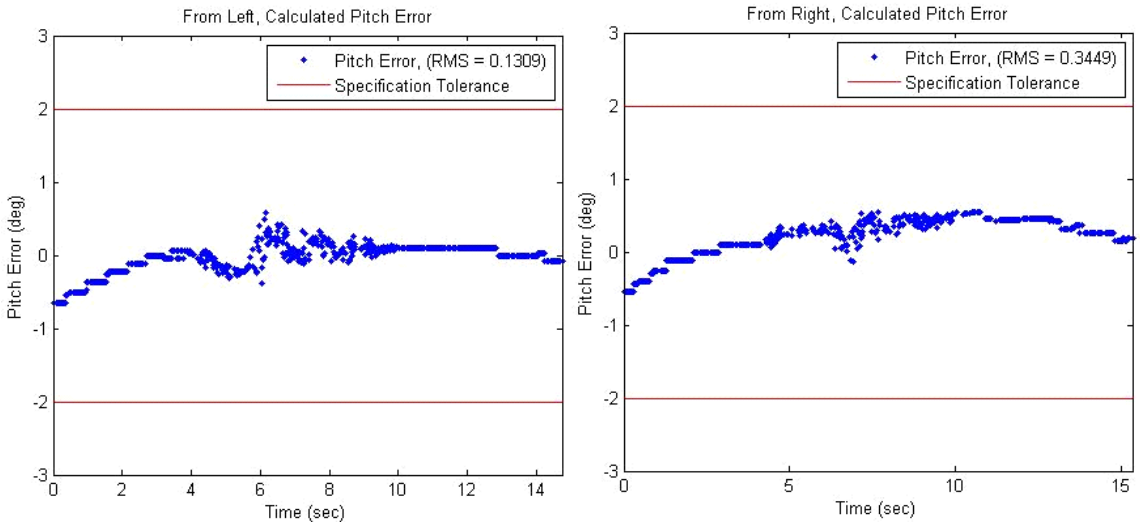

Figure 19. MTx pitch accuracy for the free swing low reference angle test.

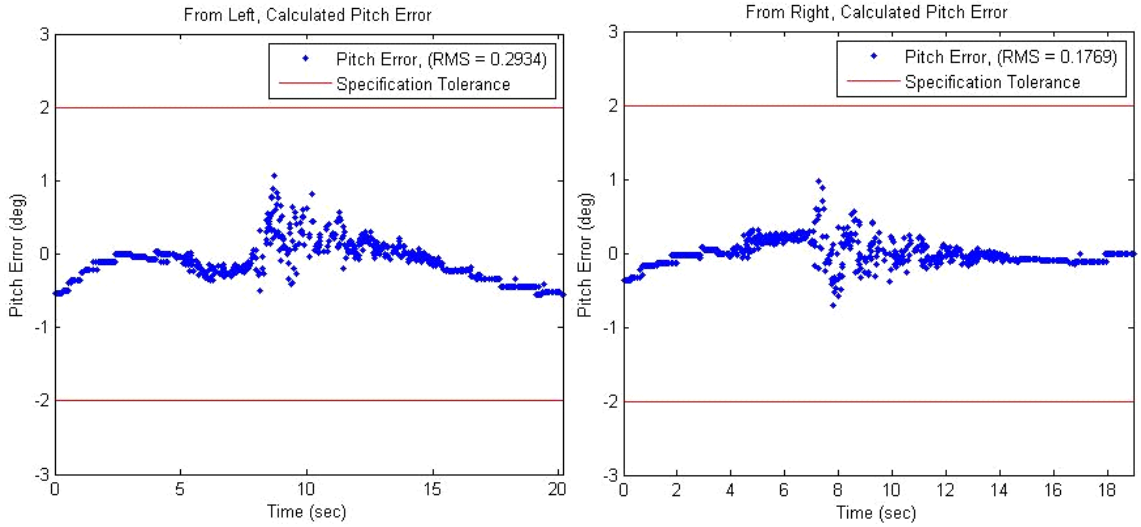

Figure 20. MTx pitch accuracy for the free swing medium reference angle test.

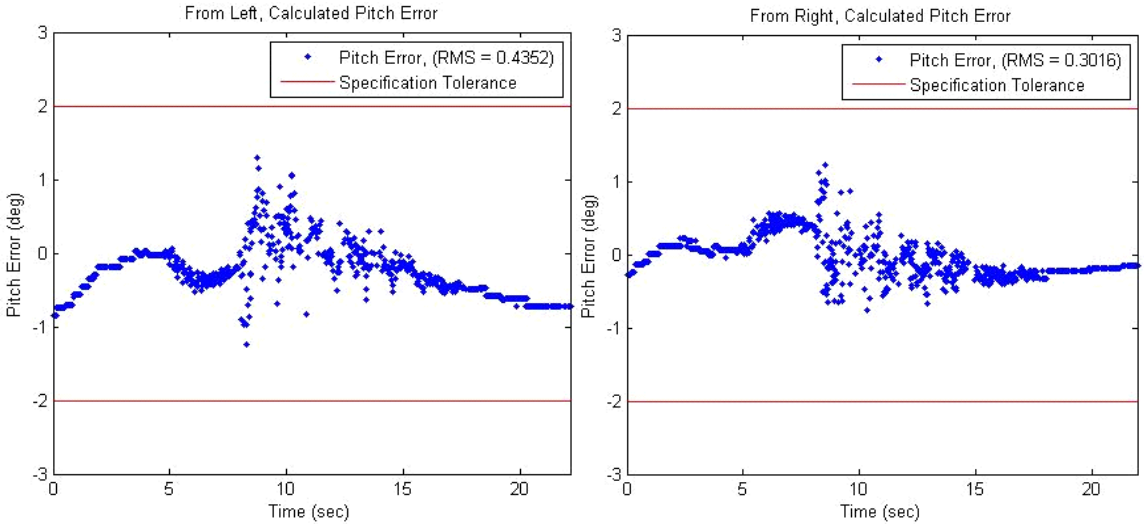

Figure 21. MTx pitch accuracy for the free swing high reference angle test.

c. Yaw

The yaw accuracy of the MTx for the free swing tests at low, medium, and high reference angles is shown in Figures 22, 23, and 24. For the low reference angle tests starting from the left and right shown in Figure 22, the RMS error was, respectively, 0.9088 degrees and 1.421 degrees and met the manufacturer specifications of 2.0 degrees. However, it is seen that the instantaneous yaw angle error reached as high as 2.0 degrees towards the end of the test starting from the right.

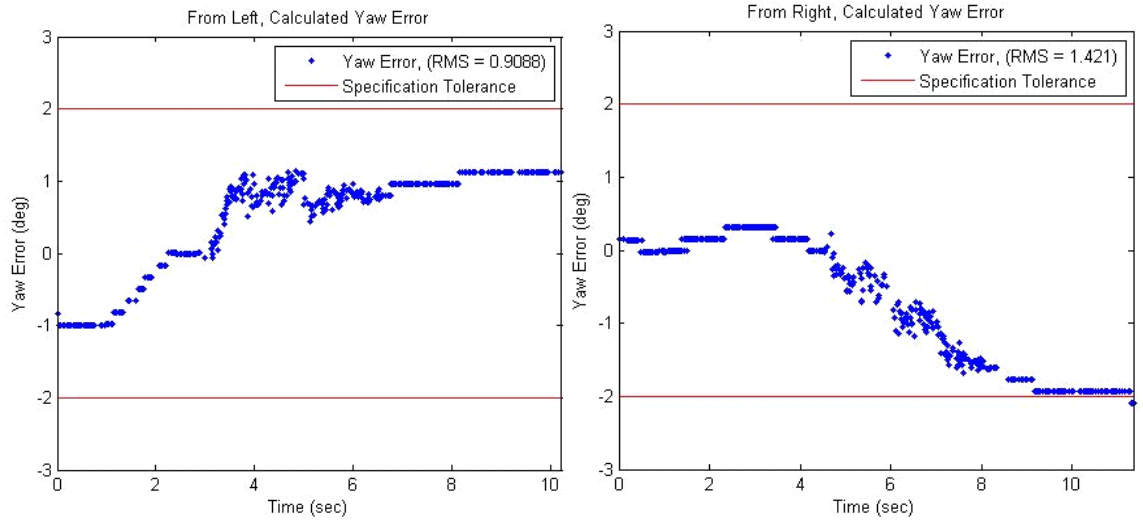

Figure 22. MTx yaw accuracy for the free swing low reference angle test.

Similar to the low reference angle results, the RMS error specification was met for both tests from the right and left, but the yaw angle exceeded the instantaneous error for the medium reference angle test starting from the right shown in Figure 23.

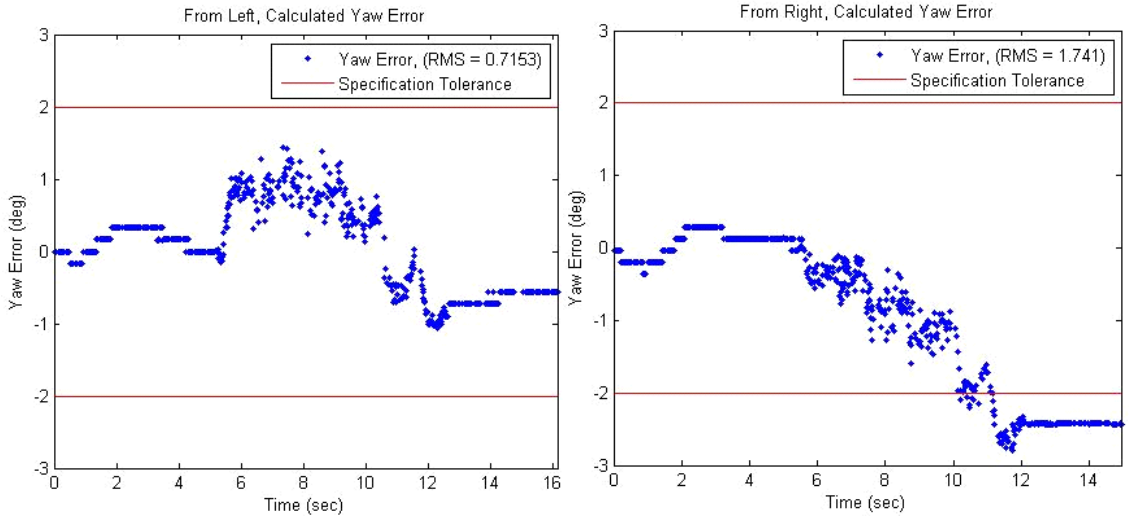

Figure 23. MTx yaw accuracy for the free swing medium reference angle test.

Finally, in the free swing high reference angle tests, the RMS error specification was met, but the yaw angle again exceeded the instantaneous error specification. Due to the pendulum position for the yaw tests, shown in Figure 8, the higher reference angle starting position does not mean the pendulum motion was faster and thus cannot be used for comparison of the different reference angle tests.

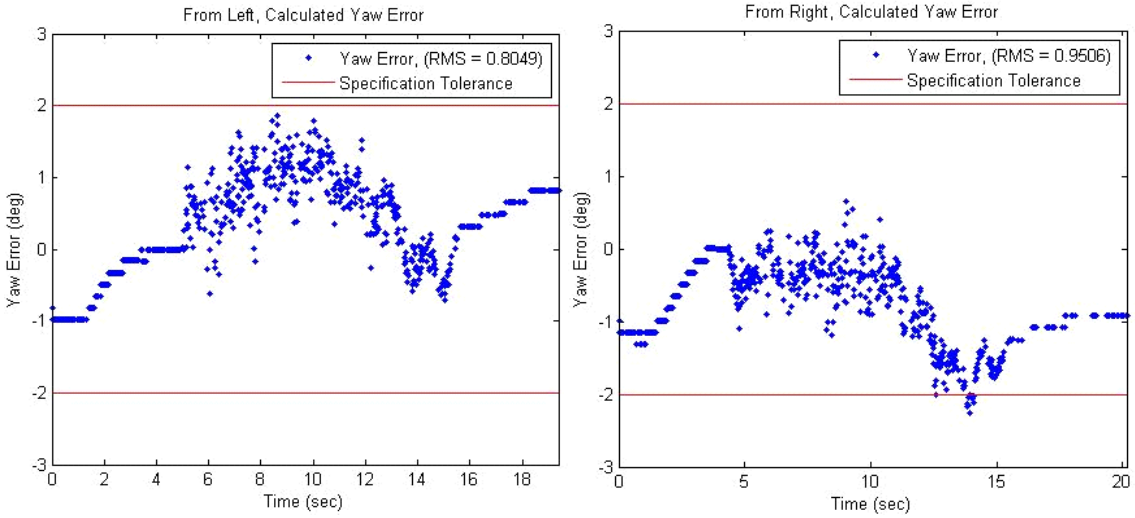

Figure 24. MTx yaw accuracy for the free swing high reference angle test.

d. Free Swing Cross-Talk

Free swing cross-talk for roll, pitch, and yaw angles under test is shown in Figures 25, 26, and 27. In all of the cross-talk figures, there was no more than seven degrees of change in the two axes that were not under test. A possible cause for the other two axes not remaining constant as expected could have been due to the placement of the MTx on the pendulum. If the rotational axis of the MTx under test was not aligned with the pendulum axis of rotation exactly, this would result in cross-talk or rotation about the other two axes. Another cause may have been that the MTx axes themselves were not aligned correctly. It could also be a combination of the two, but unfortunately, we do not have sufficient information to make a final judgment.

In Figure 25, the blue curve represents the free swing motion of the roll angle. The pitch and yaw angles are shown by green and red curves. Ideally, the pitch angle (green curve) should stay constant at zero degrees, and the yaw angle (red curve) should stay constant. However, as explained above, small deviations are visible in both pitch and yaw angles. The deviation of the yaw angle is even more profound in the pitch free swing test as depicted by the red curve in Figure 26.

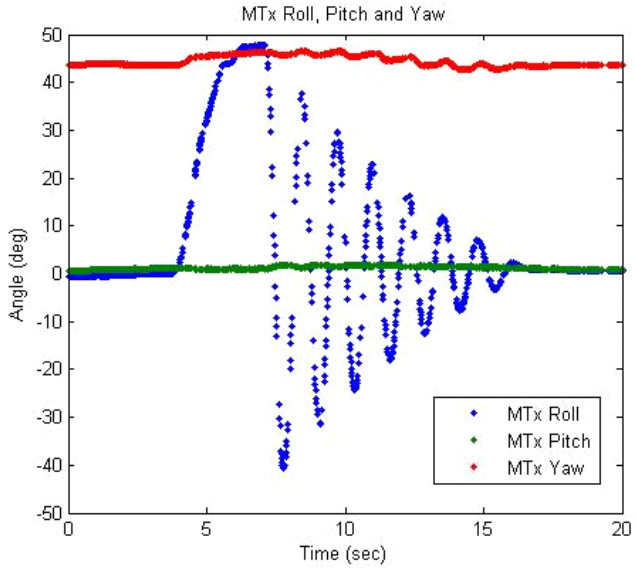

Figure 25. MTx cross-talk for the roll free swing high reference test.

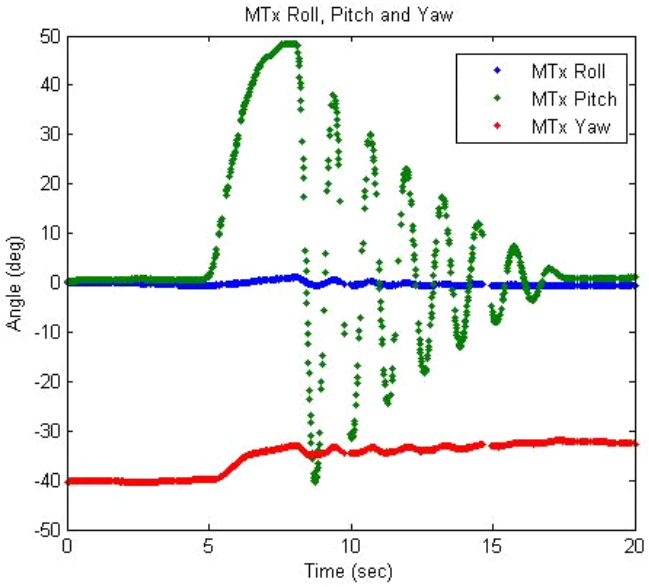

Figure 26. MTx cross-talk for the pitch free swing high reference test.

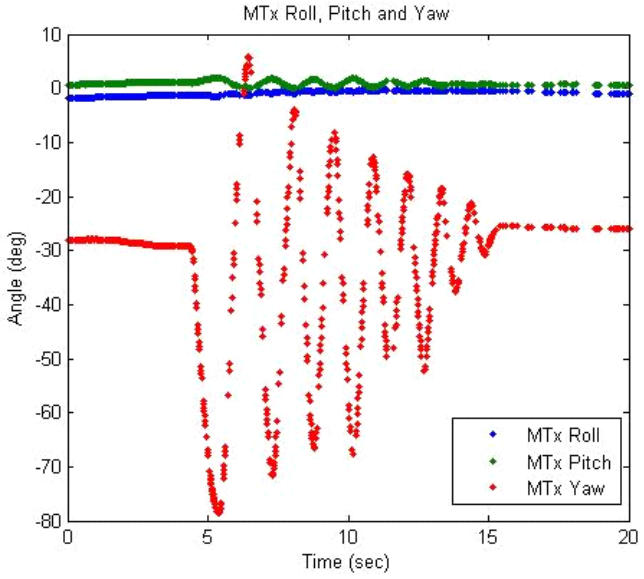

Figure 27. MTx cross-talk for the yaw free swing high reference test.

2. Arbitrary Movement

This section contains the results of the arbitrary movement tests described in Chapter III for roll, pitch, and yaw angles of the MTx.

a. Roll

The roll accuracy of the MTx for the arbitrary movement test is shown in Figure 28. The roll angle met both the RMS and instantaneous error specifications in the arbitrary movement test.

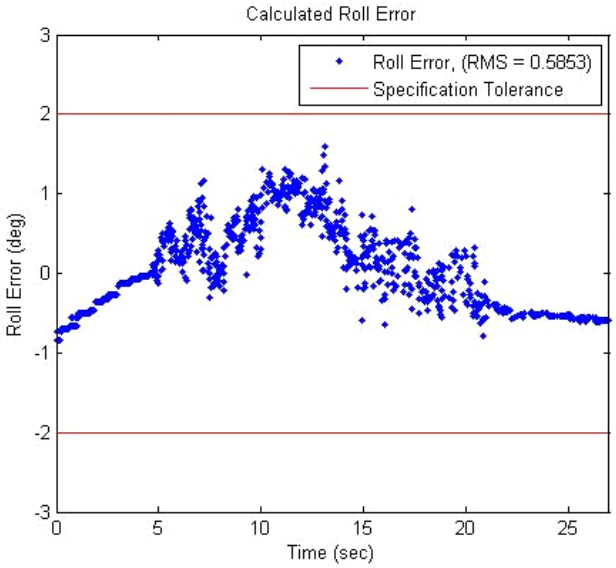

Figure 28. MTx roll accuracy for the arbitrary movement test.

b. Pitch

The pitch accuracy of the MTx for the arbitrary movement test is shown in Figure 29. Similar to the roll accuracy, the pitch also met both specifications.

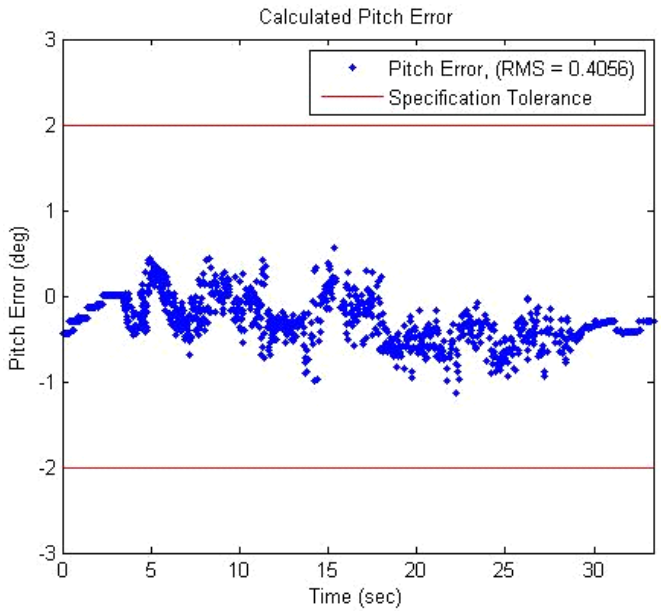

Figure 29. MTx pitch accuracy for the arbitrary movement test.

c. Yaw

The yaw accuracy of the MTx for the arbitrary movement test is shown in Figure 30. Unlike the roll and the pitch, the yaw angle did not meet either of the RMS or the instantaneous error specification. The error increased during the period of motion, which indicates that the yaw angle was drifting. This is an important finding that prompted more detailed investigation of the yaw angle performance reported in subsections 5 and 6 as well as the investigation of another inertial sensor reported in section C.

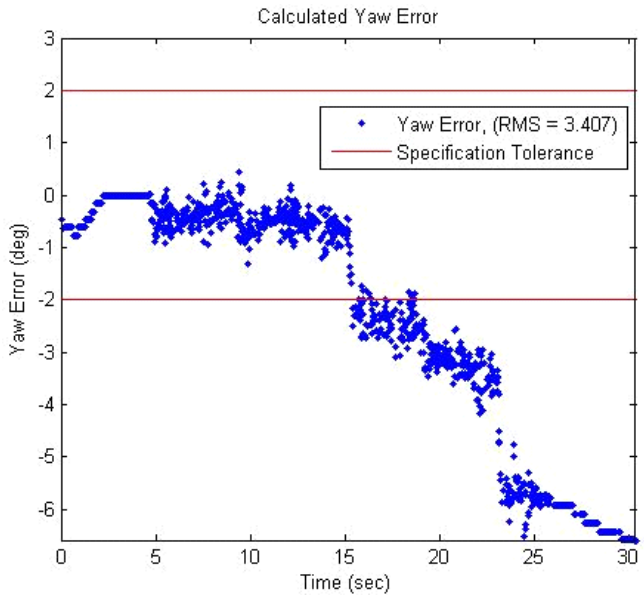

Figure 30. MTx yaw accuracy for the arbitrary movement test.

3. Slow Movement

This section contains the results of the slow movement tests described in Chapter III for roll, pitch, and yaw angles of the MTx.

a. Roll

The roll accuracy of the MTx for the slow movement test is shown in Figure 31. The roll angle met both RMS and instantaneous error specifications in the slow movement test.

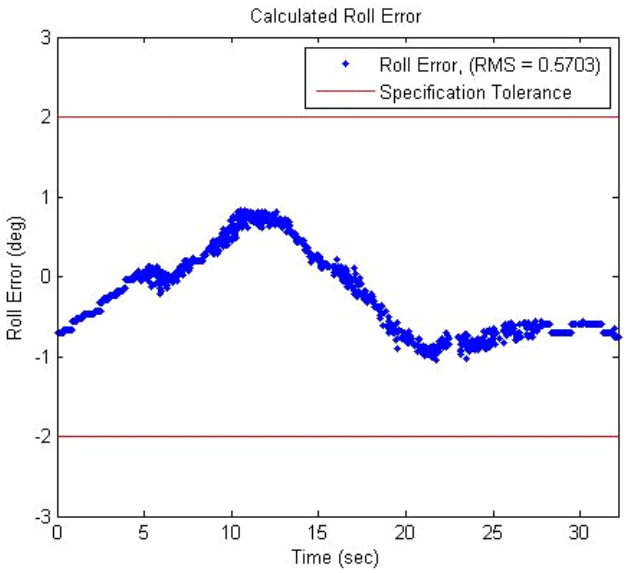

Figure 31. MTx roll accuracy for the slow movement test.

b. Pitch

The pitch accuracy of the MTx for the slow movement test is shown in Figure 32. Similar to the roll angle, the pitch angle also met both errors specifications for the test.

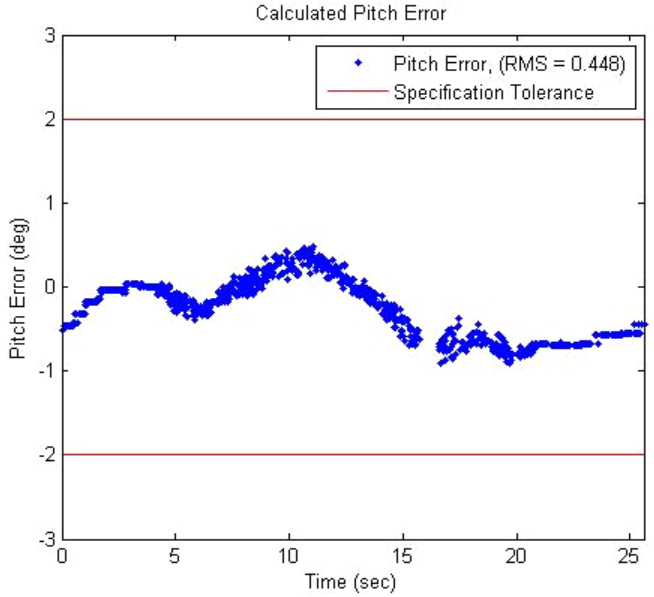

Figure 32. MTx pitch accuracy for the slow movement test.

c. Yaw

The yaw accuracy of the MTx for the slow movement test is shown in Figure 33. The yaw angle also met both error specifications. Comparing Figure 33 and the results from the arbitrary movement test in Figure 30, which contained faster motion than the slow movement test, we can conclude that the MTx yaw angle was able to track slower motion of the pendulum better than faster motion of the pendulum.

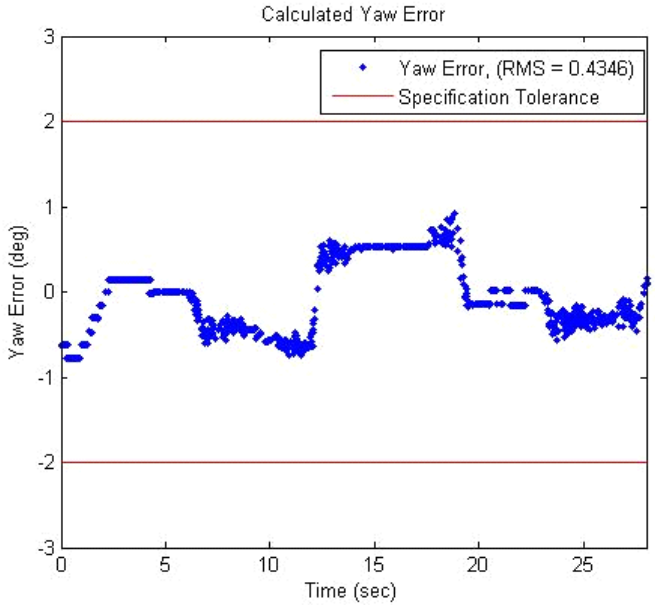

Figure 33. MTx yaw accuracy for the slow movement test.

4. Stop and Hold

This section contains the results of the stop and hold tests described in Chapter III for roll, pitch, and yaw angles of the MTx.

a. Roll

The roll accuracy of the MTx for the stop and hold test is shown in Figure 34. The roll angle met the RMS and instantaneous error specifications for the stop and hold test.

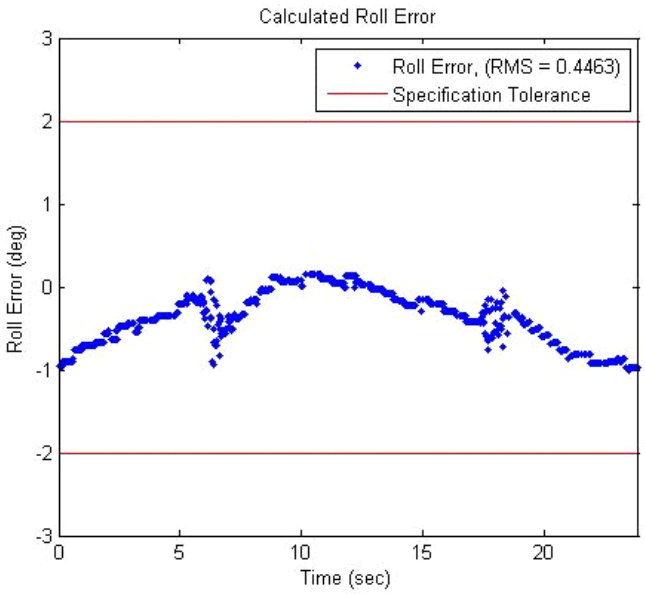

Figure 34. MTx roll accuracy for the stop and hold test.

b. Pitch

The pitch accuracy of the MTx for the stop and hold test is shown in Figure 35. The pitch angle also met both error specifications.

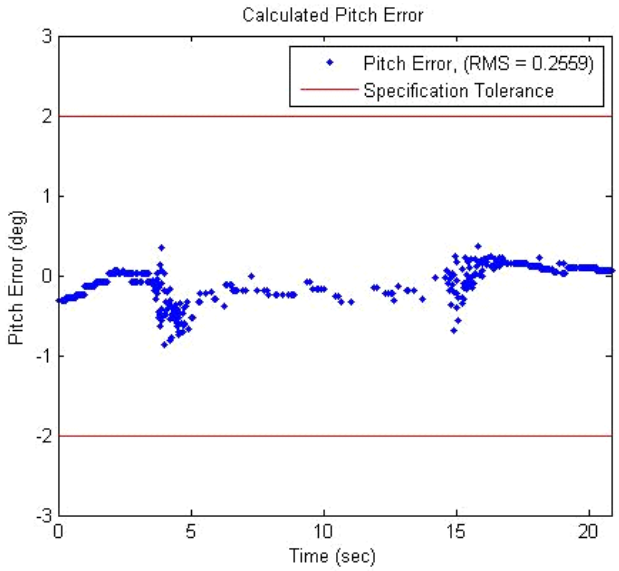

Figure 35. MTx pitch accuracy for the stop and hold test.

c. Yaw

The yaw accuracy of the MTx for the stop and hold test is shown in Figure 36. Similar to the roll and pitch angles, the yaw angle also met both error specifications.

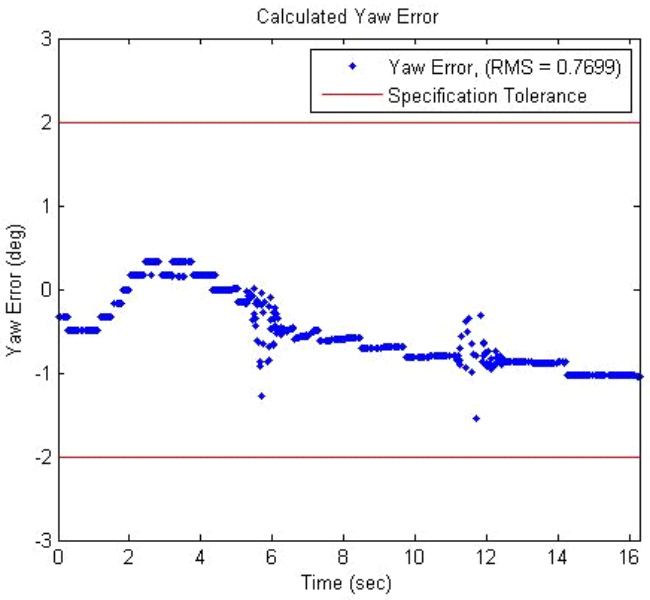

Figure 36. MTx yaw accuracy for the stop and hold test.

5. Longer Arbitrary Movement

This section contains the results of the longer arbitrary movement tests described in Chapter III for roll, pitch, and yaw angles of the MTx. When the arbitrary movement test was conducted, it was observed that the yaw angle tended to drift. That test was conducted for a short duration of 30 seconds. To further investigate the issue, a longer arbitrary movement test was carried out.

a. Roll

The roll accuracy of the MTx for the longer arbitrary movement test is shown in Figure 37. The roll angle met both RMS and instantaneous error specifications for the longer arbitrary movement test.

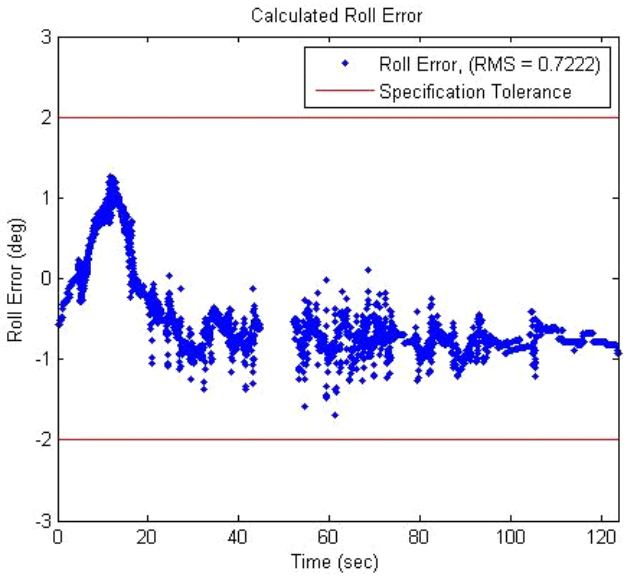

Figure 37. MTx roll accuracy for the longer arbitrary movement test.

b. Pitch

The pitch accuracy of the MTx for the longer arbitrary movement test is shown in Figure 38. Similar to the roll angle, the pitch angle also met both error specifications.

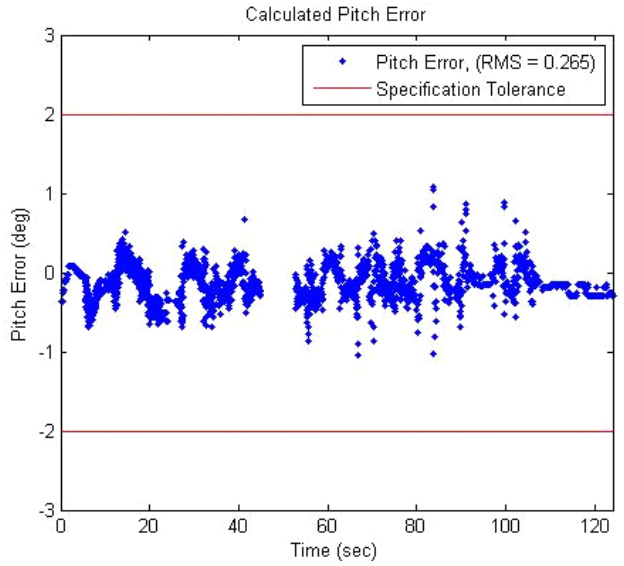

Figure 38. MTx pitch accuracy for the longer arbitrary movement test.

c. Yaw

The yaw accuracy of the MTx for the longer arbitrary movement test is shown in Figure 39. Just as in the arbitrary movement test, the yaw angle did not meet the RMS or the instantaneous error specifications for the longer arbitrary movement test. This test shows the error increasing throughout the period of motion and then decreasing after the motion stops when the MTx was static.

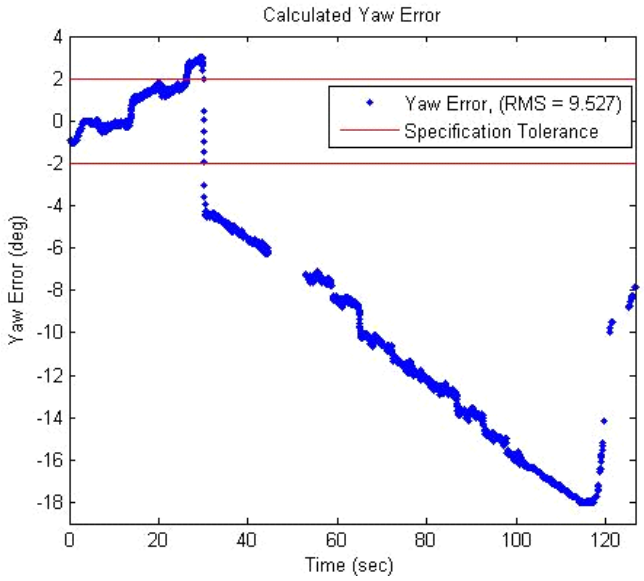

Figure 39. MTx yaw accuracy for the longer arbitrary movement test.

6. Additional Yaw Tests

This section contains the results of the additional yaw tests described in Chapter III.

a. Static

The yaw angle of the MTx for the static test is shown in Figure 40. This static test of the yaw angle shows that the yaw angle did not drift when the MTx was not in motion.

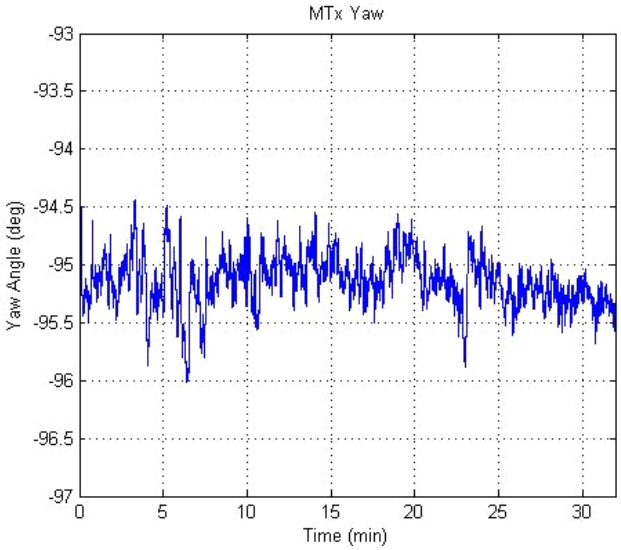

Figure 40. MTx yaw angle for the static test.

b. Three Minute Arbitrary

The yaw accuracy of the MTx for the three minute arbitrary movement test is shown in Figure 41. A plot of the MTx yaw angle and encoder angle along with the error plot are contained in Figure 41. The plot of the yaw and encoder angle shows that the MTx yaw angle did drift during a period of constant motion. Another indication that the yaw angle drifted was the error constantly increasing during the motion test.

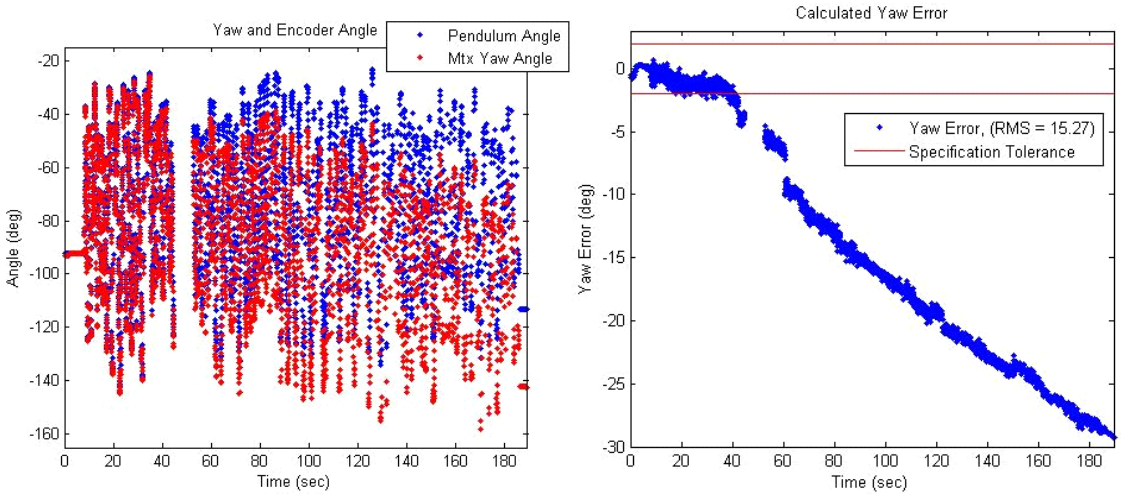

Figure 41. MTx yaw accuracy for the three minute arbitrary movement test.

c. Long Arbitrary with Stop

The yaw accuracy of the MTx for the long arbitrary movement with stop test is shown in Figure 42. The MTx yaw angle and encoder angle along with the error plot are contained in Figure 42. As was seen in the three minute arbitrary test, during the first minutes of this test the error constantly increased and the yaw angle drifted. Once motion was stopped and the MTx was static, the yaw angle converged to a value within the instantaneous specification. This convergence shows that the yaw angle when static met the instantaneous error specification.

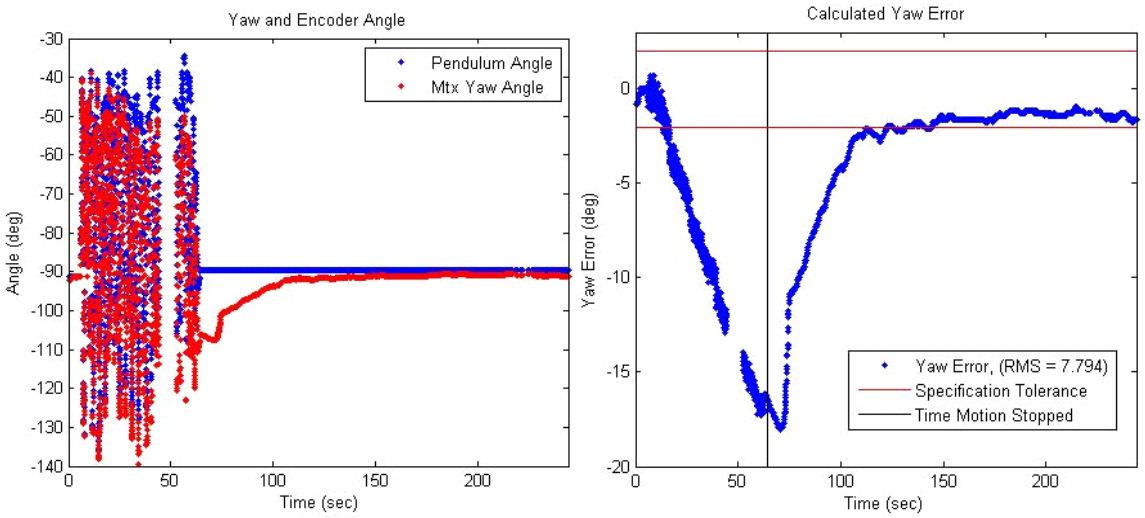

Figure 42. MTx yaw accuracy for the longer arbitrary movement with stop test.

C. 3DM-GX3 RESULTS

This section contains results of the additional yaw tests described in Chapter III conducted on the 3DM-GX3. The results are displayed in the form of error plots. Motivated by the yaw angle drift of MTx observed in the previous section, additional yaw tests were conducted on another sensor, namely 3DM-GX3. The purpose was to determine if the drift is unique to MTx or not.

1. Slow Movement

The yaw accuracy of the GX3 for the slow movement test is shown in Figure 43. A plot of the GX3 yaw angle and encoder angle as well as the respective error

plot are contained in Figure 43. The yaw angle met the RMS error specification but not the instantaneous error specification for the slow movement test.

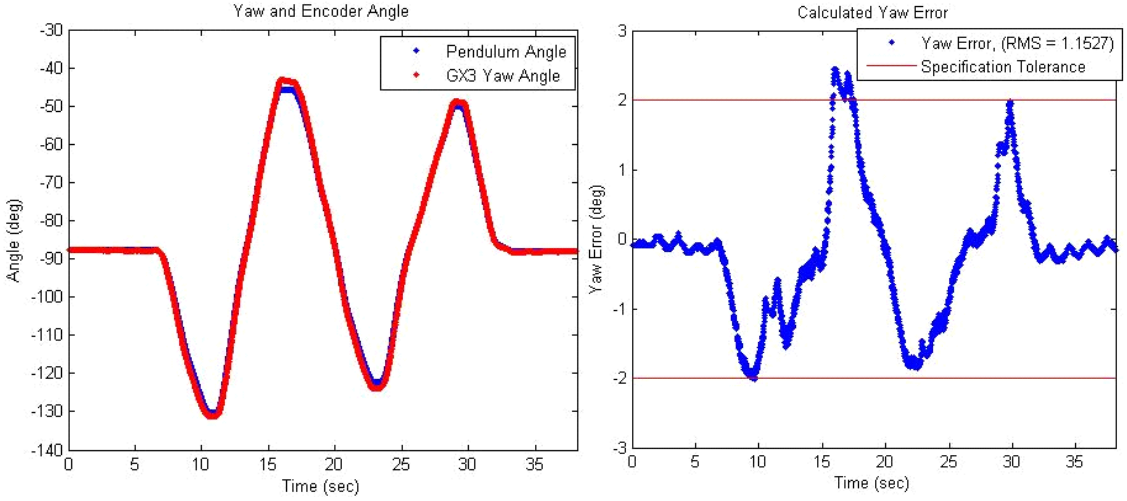

Figure 43. 3DM-GX3 yaw accuracy for the slow movement test.

2. Short Arbitrary

The yaw accuracy of the GX3 for the short arbitrary movement test is shown in Figure 44. A plot of the GX3 yaw angle and encoder angle as well as the respective error plot are contained in Figure 44. The yaw angle did not meet either error specification for the short arbitrary movement test. The yaw angle error plot shows spikes in the error under constant motion unlike the constantly increasing error of the MTx yaw angle. Once the GX3 was static, the yaw angle was within the instantaneous error specification similar to the results of the MTx yaw angle.

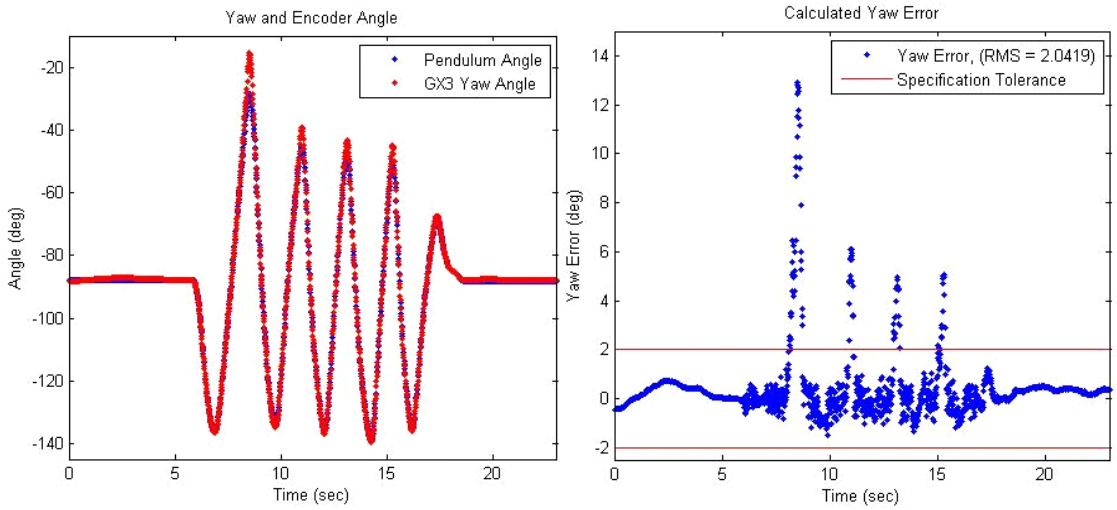

Figure 44. 3DM-GX3 yaw accuracy for the short arbitrary movement test.

3. Long Arbitrary

The yaw accuracy of the GX3 for the long arbitrary movement test is shown in Figure 45. A plot of the GX3 yaw angle and encoder angle as well as the respective error plot are contained in Figure 45. The longer arbitrary test shows the same results as the short arbitrary test. The GX3 yaw angle did not drift but instead had large instantaneous error values. The slower movement test conducted on the GX3 had much lower instantaneous error values than the arbitrary movement tests which contained faster motion. Like the MTx yaw angle, the GX3 yaw angle also tracked slower movement better than faster movement.

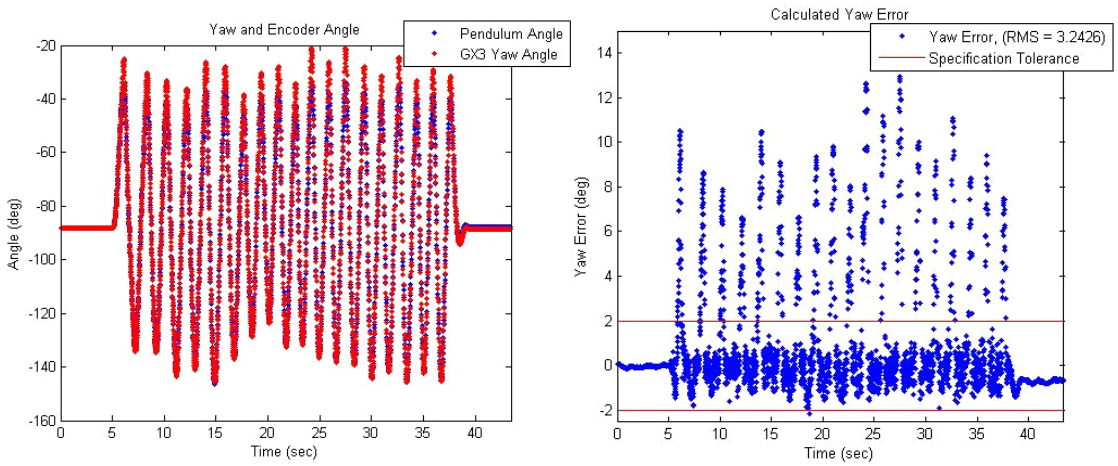

Figure 45. 3DM-GX3 yaw accuracy for the long arbitrary movement test.

D. OBSERVATIONS

Based on all of the data collected, the MTx performed well and met the manufacturer RMS dynamic accuracy specification most of the time. There was minimal cross-talk seen for the roll, pitch, or yaw angle under test. The MTx rotation angles showed higher instantaneous errors for tests involving faster motion.

For all of the tests, the MTx roll and pitch angles were within the RMS dynamic accuracy specification as well as the instantaneous ±2 degree accuracy needed for human motion tracking. The yaw angle was within the RMS dynamic accuracy specification for most of the tests that lasted less than a minute and at times had an instantaneous error that exceeded ±2 degrees. During the first test that lasted for over a minute, we observed a trend in the yaw error. The trend can be seen in Figure 39, where the error was increasing during motion due to the yaw angle drift.

To further investigate the causes of this trend, additional tests were performed on the MTx yaw angle. First a static test was performed to see if the yaw angle drifted during no motion. Drift during the static test would indicate that the magnetometers were the source of the yaw angle drift since they are the primary component used to calculate heading or yaw angle during no motion. It can be concluded from this test that the

magnetometers were not the source of the drift during motion because the yaw angle did not drift during the static test. The yaw angle drift was due instead to the algorithm that calculated the yaw angle during motion.

The final two additional tests conducted on the MTx showed that during continuous back and forth motion the yaw angle error increased constantly. Once the motion stopped, the algorithm settled on a yaw angle that was within ±2 degrees of the encoder truth angle.

The GX3 displayed certain trends in yaw error in the additional tests performed. During the slow movement test, the GX3 was within the two degree RMS error specification but at times did not stay within ±2 degrees of the encoder truth angle. The short and long arbitrary movement tests resulted in a RMS error which exceeded the two degree specification. In both of these tests, the GX3 yaw angle had error spikes when the pendulum abruptly changed motion. The GX3 yaw angle also performed much better in slower movement tests versus faster movement tests. The yaw error seen in slower movement tests versus faster movement tests was consistent with the yaw angle results of the MTx. The GX3 and MTx both showed that during faster motion the yaw accuracy was worse than during slower motion. The GX3 yaw angle did not show the same drift that was seen in the longer MTx yaw angle tests.

V. CONCLUSIONS AND RECOMMENDATIONS

A. ACCOMPLISHMENTS

In this thesis, the dynamic accuracy of an MEMS inertial sensor was investigated. The inertial sensor under test was the Xsens MTx. The MTx was integrated into an existing test apparatus by making necessary changes to an existing data collection program and attaching the sensor to the test apparatus with a mounting bracket. A test methodology was developed using tests similar to those in [10] plus some additional tests. The motion tests developed were used to investigate the dynamic accuracy of the MTx for human motion tracking applications. The accuracy was measured in the form of a RMS error value as well as instantaneous error for roll, pitch, and yaw orientation angles. A couple of tests were also conducted on the GX3 yaw angle.

The results from all of the tests conducted using the MTx showed that the roll and pitch angles met the manufacturer RMS dynamic accuracy specification, but this was not the case with the yaw angle. Similarly, the roll and pitch angles also met defined instantaneous error specifications for all tests, whereas the yaw angle did not. Further yaw angle tests on the MTx showed that the yaw angle was statically accurate but drifted during continuous back and forth motion. The results of the tests conducted on the GX3 yaw angle did not show the same drift as was the case with the MTx. Though the GX3 yaw angle did not drift, it still did not meet the dynamic error specifications.

A possible application for the MTx is human head motion tracking. The MTx roll and pitch angle accuracy are well within what is needed for human head motion tracking. The yaw angle when not under continuous back and forth motion is also suitable for human head motion tracking. Overall, the Xsens MTx could be used for human head motion tracking or other applications that do not involve continuous back and forth motion.

B. FUTURE WORK

Though all of the goals of this thesis were accomplished, there is still much work pertaining to IMUs that can be done. Only two IMUs were tested in this thesis; however,

there are many other inertial sensors that could be tested. Investigation of the accuracy of different sensors using the existing test apparatus could be conducted. Testing other sensors would also further validate that the current pendulum test apparatus is a valid method for the testing of orientation data collected from IMUs.

Another opportunity for future work would be to improve the existing data collection program. Currently, the program works but the longer it runs, the slower the data collection loop is executed. This is due to the memory allocation that is currently used on the CompactRIO, which requires the sensors to be in polling mode instead of at a set sampling frequency. Changing the program so that the sensor can be sampled at a set frequency would be more realistic of how the sensor would be used in an application.

Lastly, the current test apparatus only allows for testing of one rotation angle at a time. This may not be realistic enough for certain applications. Thus, development of a test apparatus that would allow for testing of two or all three rotation angles at a time is desirable.

APPENDIX. LABVIEW DIAGRAMS

This Appendix contains the two LabVIEW subVIs presented in this thesis. The MTx initialization subVI is contained in Figure 46. This subVI shows that actual VIs used in LabVIEW to initialize the MTx output settings.

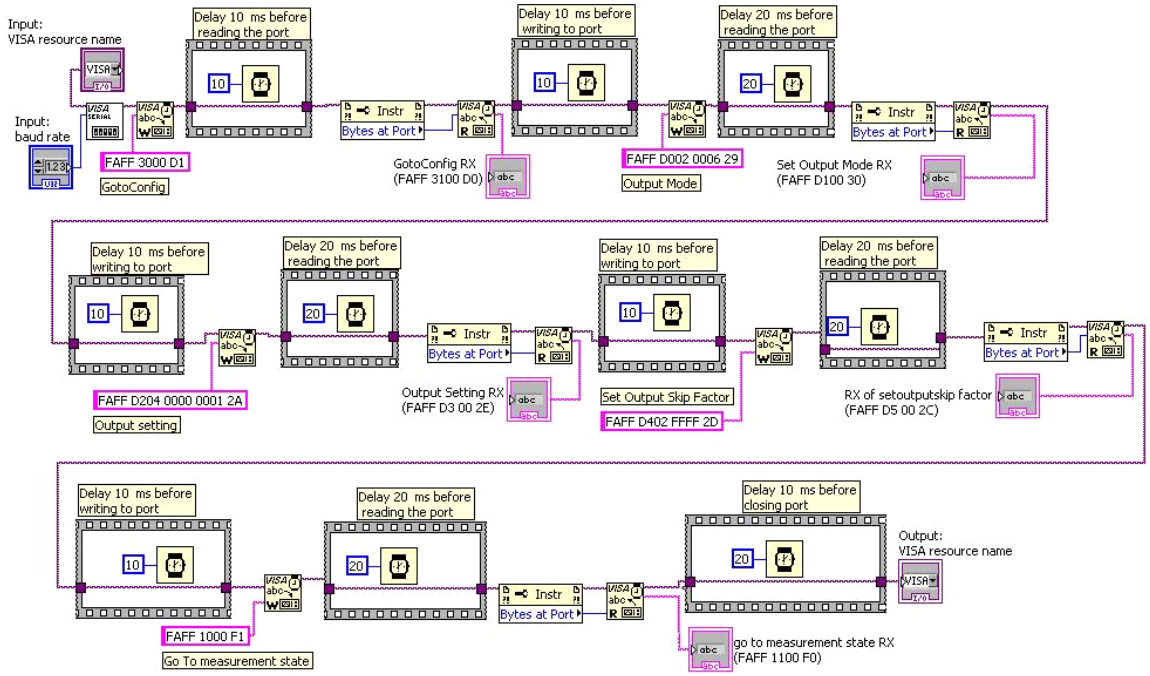

Figure 46. MTx serial initialization subVI.

The MTx data collection subVI is shown in Figure 47. This subVI shows all of the VIs used to request, receive, and process data from the MTx.

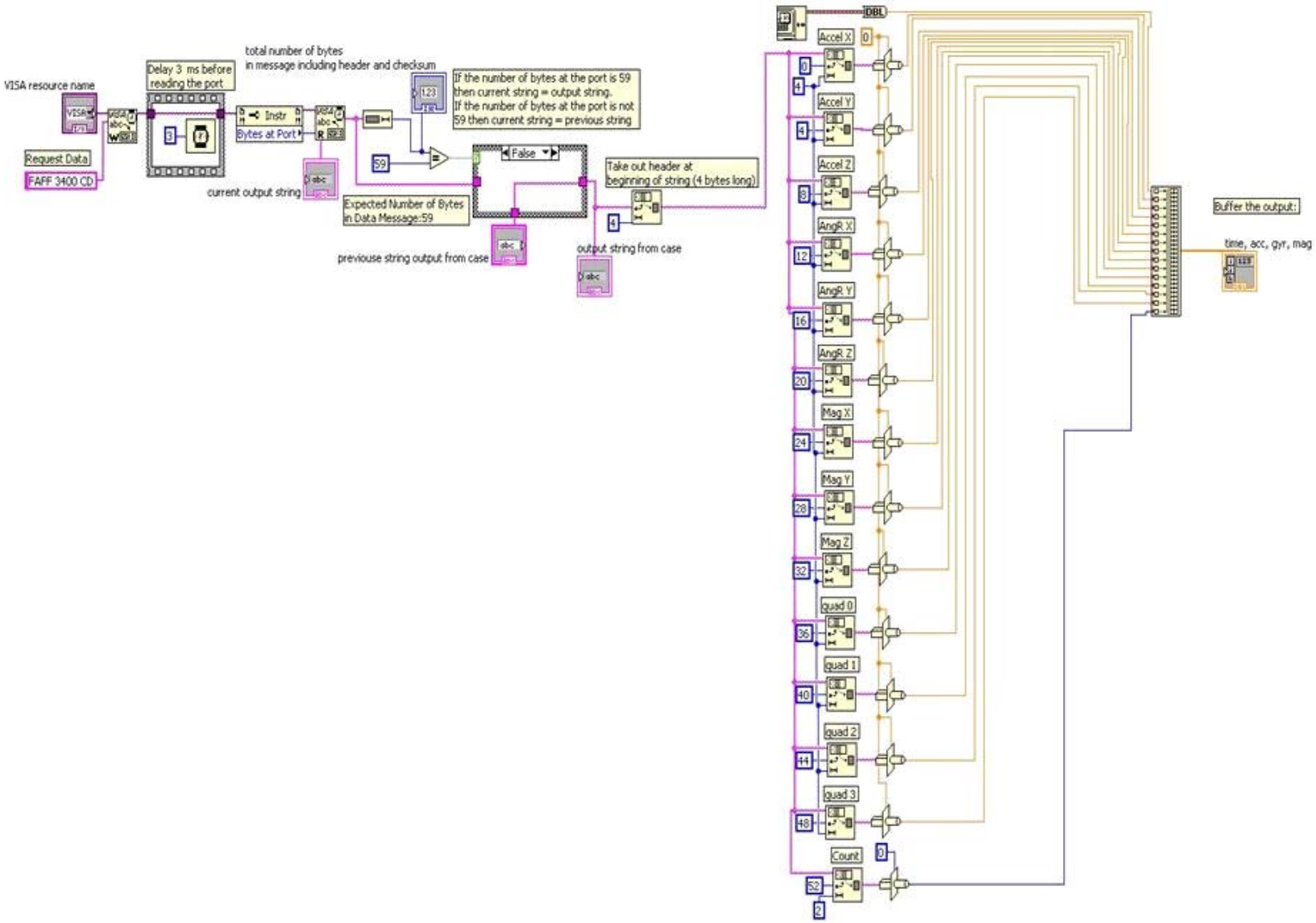

Figure 47. MTx data collection subVI.

LIST OF REFERENCES

[1] "Micro-electro-mechanical systems (MEMS)," *McGraw-Hill Concise Encyclopedia of Science and Technology*. New York: McGraw-Hill, 2006, *Credo Reference*, [Online]. Available: http://www.credoreference.com/entry/conscitech/micro_electro_mechanical_systems_mems, [Accessed: February 29, 2012].

[2] Xsens Technologies B.V., "Xsens MVN – inertial motion capture," [Online]. Available: http://www.xsens.com/en/general/mvn, [Accessed: February 27, 2012].

[3] J. Calusdian, "A personal navigation system based on inertial and magnetic field measurements," PhD dissertation, Naval Postgraduate School, Monterey, CA, September 2010.

[4] "Inertial navigation system." McGraw-Hill Concise Encyclopedia of Science and *Technology*. New York: McGraw-Hill, 2006, *Credo Reference*, [Online]. Available: http://www.credoreference.com/entry/conscitech/inertial_navigation system, [Accessed: February 29, 2012].

[5] IEEE Std 1554-2005, *IEEE Recommended Practice for Inertial Sensor Test Equipment, Instrumentation, Data Acquisition, and Analysis*, New York, NY, IEEE, 2005.

[6] A. Kealy, G. Roberts, and G. Retscher, "Evaluating the performance of low cost MEMS inertial sensors for seamless indoor/outdoor navigation," *IEEE Position Location and Navigation Symposium*, May 2010, pp. 157–167.

[7] H. Harms, O. Amft, R. Winkler, J. Schumm, M. Kusserow, and G. Troester, "ETHOS: Miniature orientation sensor for wearable human motion analysis," *IEEE Sensors Conference*, November 2010, pp. 1037–1042.

[8] A. G. Cutti, A. Giovanardi, L. Rocchi, and A. Davalli, "A simple test to assess the static and dynamic accuracy of an inertial sensors system for human movement analysis," *IEEE Engineering in Medicine and Biology Society International Conference*, September 2006, pp. 5912–5915.

[9] J. Shaver, "PC104 control environment development and use for testing the dynamic accuracy of the MicroStrain 3DM-GX1 sensor," M.S. thesis, Naval Postgraduate School, Monterey, CA, June 2007.

[10] J. Cookson, “A method for testing the dynamic accuracy of micro-electro-mechanical systems (MEMS) magnetic, angular rate, and gravity (MARG) sensors for inertial navigation systems (INS) and human motion tracking applications,” M.S. thesis, Naval Postgraduate School, Monterey, CA, June 2010.

[11] *MTi and MTx User Manual and Technical Documentation*, Xsens Technologies B.V., October 2010.

[12] *MT Low-Level Communication Protocol Documentation*, Xsens Technologies B.V., October 2010.

[13] J. B. Kuipers, *Quaternions and Rotation Sequences*. New Jersey: Princeton University Press, 1999.

[14] “Root-mean-square.” McGraw-Hill Concise Encyclopedia of Science and *Technology*, New York: McGraw-Hill, 2006. *Credo Reference*, [Online]. Available: http://www.credoreference.com/entry/conscitech/root_mean_square, [Accessed: April 19, 2012].

INITIAL DISTRIBUTION LIST

1. Defense Technical Information Center
   Ft. Belvoir, Virginia

2. Dudley Knox Library
   Naval Postgraduate School
   Monterey, California

3. Dr. R. Clark Robertson
   Naval Postgraduate School
   Monterey, California

4. Dr. Xiaoping Yun
   Naval Postgraduate School
   Monterey, California

5. Dr. Roberto Cristi
   Naval Postgraduate School
   Monterey, California

6. ENS Leslie M. Landry
   U.S. Navy
   Franklin, Louisiana